ELSEVIER

Journal of Volcanology and Geothermal Research 110 (2001) 191–233

Journal of volcanology and geothermal research

www.elsevier.com/locate/jvolgeores

Formation of the lower ocean crust and the crystallization of gabbroic cumulates at a very slowly spreading ridge

James H. Natland[a,*], Henry J.B. Dick[b]

[a]*Rosenstiel School of Marine and Atmospheric Science, University of Miami, Miami, FL 33149, USA*
[b]*Woods hole Oceanographic Institution, Woods hole, MA 02543, USA*

Revised 25 June 2000

Abstract

Ocean Drilling Program Hole 735B was extended to 1508 m below the sea floor during Leg 176, atop a shallow bank near Atlantis II Fracture Zone on the very slowly spreading Southwest Indian Ridge. All the drilling was in gabbro, and recovery averaged nearly 87%. The drill penetrated a series of stacked plutons consisting mostly of olivine gabbro, but some with troctolite. Each pluton is some 200–500 m thick, each has its own internally coherent stratigraphy, and each apparently represents an individual event of significant magma inflation and addition to the crust. The entire column was extensively deformed along inclined zones of distributed shear before it was completely frozen, this marking the onset of unroofing of the rocks and their ascent to high rift mountains. The deformation mobilized late-stage melts into flow patterns which led to concentration of ilmenite and magnetite in hundreds of seams of oxide gabbro along or near zones of strong crystal–plastic deformation, the highly differentiated melts overall being concentrated by buoyancy forces toward the top of the section, especially in one zone nearly 70 m thick. However, upward flow was ultimately blocked or deflected by zones of impermeable rock resulting either from downward freezing or grain-size reduction during shear. A melt lens probably did not form at the base of sheeted dikes, as it does at the East Pacific Rise.

Despite this, the rocks are cumulates, and most are adcumulates, with very low residual melt porosities. Cumulate theory based on stratiform, layered intrusions does not entirely apply to these rocks. Instead, all gabbros, including the oxide gabbros, crystallized in a dense crystal mush in patterns dominated by fractures, channelized flow, and intergranular porous flow. Most gabbros are not layered; weak modal layering of uncertain origin is present in $<2\%$ of the rocks. Porosity reduction leading to formation of adcumulates at all stages was extremely efficient. This occurred in the course of synkinematic differentiation, also called differentiation by deformation, and involved compaction under conditions of lithostatic loading and shear, emplacement of crystal mushes along inclined, possibly curving faults, dissolution and reprecipitation of minerals along grain boundaries, and pressure solution, which was the final agent in porosity reduction.

As the block was lifted from beneath the rift-valley floor, crystal–plastic deformation gave way to brittle fracture, and the now dominantly subsolidus metamorphism shifted from high-temperature assemblages characterized by amphibole near the top of the section, to low-temperature assemblages with smectite–chlorite and zeolite near the bottom. The rocks acquired their stable magnetization during formation of amphiboles and secondary magnetite during this metamorphism. The entire body of rock is reversely stably magnetized at a consistent inclination, and it is rotated to the south, perhaps along a curving detachment surface, away from the ridge segment where it formed, by about 20°. It has an intensity of magnetization sufficient to account for the magnetic anomaly observed over the site.

Drilling did not reach ultramafic rock, but dredging indicates that peridotite is probably within a few hundred meters of the

* Corresponding author.
E-mail address: natland@sammy.rsmas.miami.edu (J.H. Natland).

PII: S0377-0273(01)00211-6

bottom of the hole. Seismic Moho, however, is placed at 5 km beneath the summit of Atlantis Bank. Much of the rock between Moho and the bottom of Hole 735B must therefore be partially serpentinized peridotite.

Keywords: ocean crust; gabbros; petrology; cumulates; Southwest Indian Ridge

1. Introduction

A long-standing objective of the Ocean Drilling Program has been to drill entirely through the ocean crust into the upper mantle, to see how the ocean crust is formed. Alternatively, the lower ocean crust can be sampled where faulting or erosion has removed basalts and dikes, which are difficult to drill. The high transverse ridges of major fracture zones in the Atlantic and Indian oceans have long been known as places where gabbroic and serpentinized ultramafic rock are consistently exposed to the dredge, and which therefore afford the drill a short path to the crust–mantle transition. One such location is atop a flat platform at Atlantis Bank, the eastern transverse ridge on Atlantis II Fracture Zone, Southwest Indian Ridge (Fig. 1). The bank was swath mapped in 1986 (Dick et al., 1991a) and then drilled in 1987. That section, obtained in only 720 m of water at ODP Hole 735B during Leg 118 (Robinson, Von Herzen et al., 1989) comprises 504 m of abyssal gabbro, and the hole, which was equipped with a re-entry cone atop a hard-rock base, was left open for future drilling.

The renewed drilling took place during October–December of 1997 and extended the hole to 1508 m below the sea floor (mbsf) before a sudden and unexpected drill-string failure in high seas blocked further drilling. The recovery rate of cored rock was 86.6%, virtually identical to the rate during Leg 118 (Dick, Natland, Miller et al., 1999). The section, almost entirely in gabbro, is ideal to contribute to models of crustal accretion at spreading ridges, and to compare to ophiolites, layered intrusions, and other kinds of ocean crust.

In the past, analogies of the unseen gabbroic portion of the ocean crust to the products of very different types of magma chambers have been offered (e.g. Cann, 1974; Rosendahl, 1976; Bryan and Moore, 1977; Nisbet and Fowler, 1978; Sinton and Detrick, 1992). The gabbros of Hole 735B represent one of the most complex types of magma chamber thus far discovered. Consider the following sequence. The simplest intrusion is that of a single injection of magma into some portion of the crust. Small examples are thin dikes or sills, which crystallize from quenched surfaces inward, without much internal magma movement (e.g. Marsh, 1989). A larger body, but which is still nevertheless considered to be the result of *one* injection of magma, is the Skaergaard intrusion, in which magma convected and crystallization processes were diverse (e.g. McBirney, 1996; Irvine et al., 1998). The next most complicated might be that of a steadily supplied, repetitively injected, and frequently tapped, *central* volcano, perhaps like Kilauea, as viewed from the top, but more pertinently one that produces cumulates with a repetitive sequence in both rhythmic and cryptic mineralogical variation, when considered from the interior. The best-studied example is probably Rhum, where cyclic cumulates marked by such repetitions were originally believed to have precipitated from a large, circulating, and regularly injected magma chamber (Brown, 1956; Wager and Brown, 1967). This picture has been modified by more recent field study (e.g. Bédard et al., 1988), but Rhum, perhaps more than any other place, provided a conceptual framework for considering evolution of basaltic liquids by means of crystal fractionation in recurrently replenished and tapped, fractionating (RTF) magma chambers (e.g. O'Hara, 1977; Usselman and Hodge, 1978; O'Hara and Mathews, 1981).

Some students of ophiolites postulated that variants of this type of volcano occur in the ocean crust (e.g. Greenbaum, 1972; Pallister and Hopson, 1981; Smewing et al., 1984) and this idea was taken up particularly for fast-spreading ridges (Cann, 1974; Rosendahl, 1976; Natland, 1980; Wilson et al., 1988). Besides having repetitive supply and eruption of magma, these volcanoes are also regularly and continuously rifted by sea-floor spreading, being pulled apart from top to bottom right down the middle, with each dilation of the crust volumetrically

balancing each injection of magma. The crust has little relief, and is virtually constant in thickness. However, as we now understand it, there is no large magma body beneath the axis of the East Pacific Rise (Sinton and Detrick, 1992), as indeed, there was none at Rhum (cf. Emeleus et al., 1996). Instead, drilling shows that at the East Pacific Rise, high-level cumulates, at least, form in a narrow, generally vertical or dike-like, channelized network within a crystal mush (Natland and Dick, 1996). Some melt collects at a thin and narrow sill-like lens at the base of the dikes (e.g. Kent et al., 1993) and also in another at the mantle transition (Crawford et al., 1999). This is not a simple volcano, yet it is unquestionably a common type on the Earth's surface. The activity of such a volcano can really only be understood by exploring it on the sea floor. Certainly, absence of a major magma body — an RTF magma chamber — was not a conclusion reached, at least initially, by studying layered cumulates at the supposedly fast-spread Semail ophiolite in Oman (Pallister and Hopson, 1981; Smewing et al., 1984).

Finally, add two more factors to the complexity of the series of volcanoes so far imagined, for the case of slowly spreading ocean crust. The first is that spreading and magmatic processes are, in comparison to fast-spreading ridges, *slowed down*, *irregular* and *infrequent*. They do not always even act precisely on the geometric center of spreading, but scatter around it to some extent. Although magmatism obviously contributes to the gabbroic layer, this must occur in the absence of any persistent magma body (e.g. Nisbet and Fowler, 1978; Sinton and Detrick, 1992), not even the thin melt lenses of the East Pacific Rise. These processes thus must leave a record of composite and overlapping intrusion. The second factor is that, even as this collection of intrusions is assembled, its very roots are rent asunder by tectonic forces that go far beyond those of the simple dilation experienced at a fast-spreading ridge. These forces are tied to the formation of rifted mountains. The faults intersect the consolidating magma body obliquely, and tear it apart laterally along both narrow and wide zones of high-temperature shear even while magma is being added from below. This complicated magma-chamber system is what has been unearthed at Hole 735B. There, crustal accretion occurred at the same time as severe high-temperature deformation, and magmatic differentiation acted in concert with formation of metamorphic textures in the selfsame rocks.

In 1987, at the time of Leg 118, no matter how the crust at slowly spreading ridges was thought to form, no one conceived of this. No accounts in the literature prepared us for the intimate connection between magmatism and shear that these rocks revealed. They challenged our ability even to name them, let alone break them down into a rational igneous stratigraphy. In retrospect, we can identify some places on land where counterparts may exist, and study of both ophiolites and layered intrusions has produced a few parallels and clarified some of what was puzzling in 1987. However, in overall aspect, nothing like Hole 735B has yet been described. The gabbros there, in their well-understood tectonic setting, are not merely a type section for lower ocean crust at one kind of ridge. They also represent a class of igneous rock, widespread on the Earth's surface (if only just beginning to be revealed), for which concepts of the mechanisms of magmatic differentiation and formation of cumulates, however they have been developed from the study of layered intrusions and ophiolites, either do not apply, or are in need of extension and revision. This theme is addressed from a number of perspectives in the following.

2. Setting

The Southwest Indian Ridge is nearly the slowest spreading of rises and ridges, with an average combined spreading rate of only 1.5 cm/yr for most of its length (Sclater et al., 1981; Fisher and Sclater, 1983; Patriat et al., 1997). Ridge segments are oriented east–west (Fig. 1, inset), and the easternmost segment is propagating at the Indian Ocean triple junction into the divergence produced by the different spreading directions of the Central and Southeast Indian Ridges (Patriat and Parson, 1989; Patriat et al., 1997). These have slow and intermediate rates of spreading, respectively. Large-offset transforms are spaced on the order of 100 km apart on the Southwest Indian Ridge, and asymmetric spreading apparently produced the substantial lengths of many offsets as the triple junction propagated relatively toward the east. This is the simplest way to explain

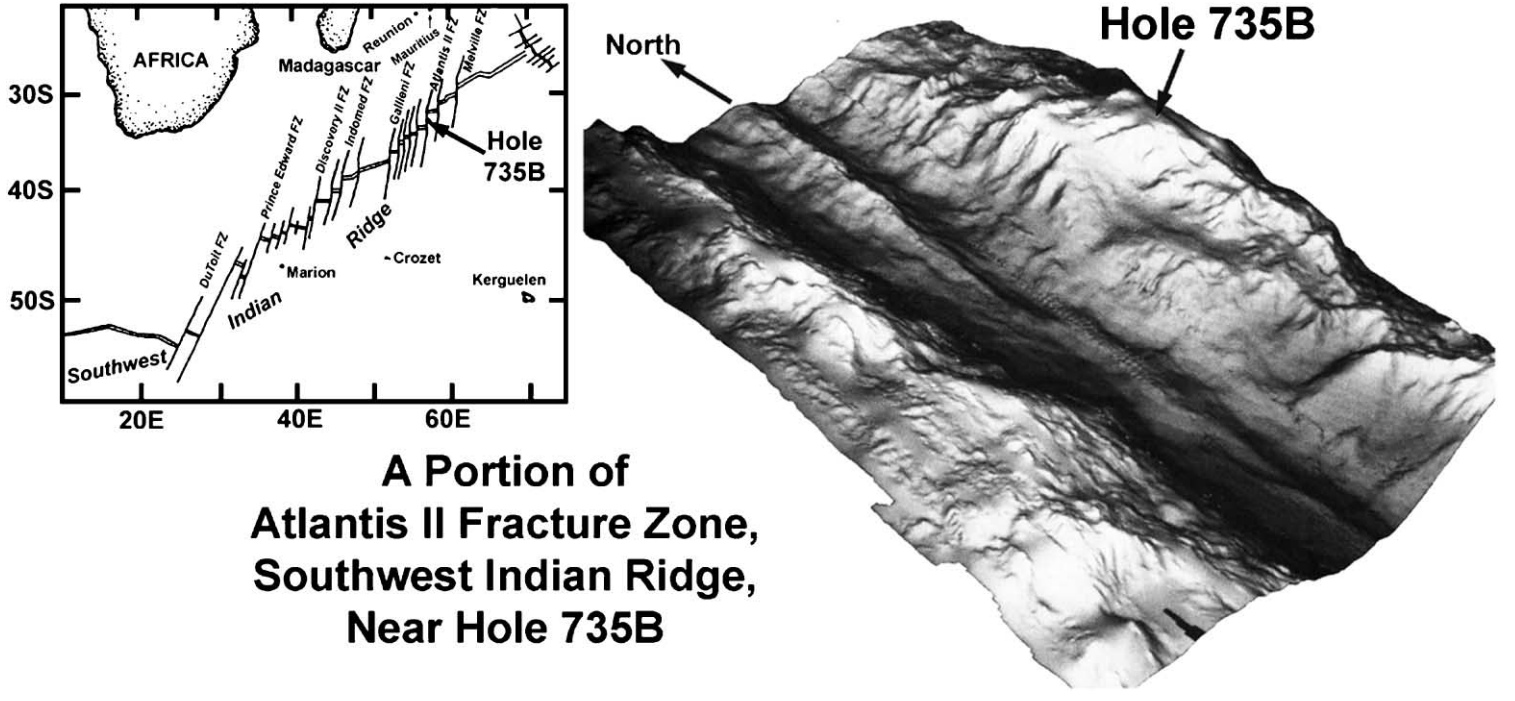

Fig. 1. Location of Hole 735B on the Southwest Indian Ridge, and an oblique shaded-relief image of a portion of the Atlantis II Fracture Zone transform valley, showing Atlantis Bank, where Hole 735B was drilled. The relief image, from the frontispiece of *Proc. ODP, 118, Scientific Results* (Von Herzen et al., 1991), is based on a SeaBeam survey carried out in 1986 (Dick et al., 1991A), and represents an area of about 4000 km^2. Hole 735B is in 720 m of water, and the floor of the transform valley is about 6000 m deep.

how the ridge segments came to span more than 30° of latitude. For Atlantis II Fracture Zone, asymmetric spreading, documented by analysis of magnetic anomalies, has lengthened the transform fault by about 0.4 cm/yr (Dick et al., 1991a). The rocks of Hole 735B occupied the rift valley to the north at about 11.5 Ma.

The transform portion of Atlantis II Fracture Zone has high transverse ridges on both sides (Dick et al., 1991a), like many major fracture zones on deeply rifted, slowly spreading ridges. Transform faults at DuToit and Discovery II Fracture Zones on the Southwest Indian Ridge, and Argo, Vema and Marie Celeste Fracture Zones on the Central Indian Ridge, have transverse ridges that reach to within less than 1 km of sea level, or some 4–5 km higher than adjacent rift and transform valleys (Engel and Fisher, 1975; Fisher et al., 1986). There is not yet a satisfactory explanation for the extent of these uplifts, but they are clearly tied to the formation of rifted mountains, with the relief being accentuated near transform faults. Gabbro and serpentinized peridotite are quite typically dredged from all structural levels of transverse ridges in the Indian Ocean (e.g. Fisher et al., 1986; Dick, 1989; Dick et al., 1991a). Basalts and dikes that once covered them on the rift-valley floor were evidently removed by faulting. Since ultramafic rocks occur even on the tops of transverse ridges, including Atlantis Bank (Dick et al., 1999), vertical displacements of 6–10 km consequently are inferred. The spacing of blocks between the major displacements is still unknown. Plutonic assemblages on the walls of transform valleys in the Indian Ocean (Engel and Fisher, 1975; Fisher et al., 1986) and in the North Atlantic (e.g. Cannat, 1993; Lagabrielle et al., 1998; Karson, 1998) indicate that basalts and dikes were separated from gabbroic and ultramafic rock mainly in an assymetric fashion and probably along inclined or curving faults reaching deep beneath the rift valley. The portion of Hole 735B drilled during Leg 118 penetrated shear zones expressing such faulting in originally high-temperature and still ductile igneous material (Dick et al., 1991a; Bloomer et al., 1991; Natland et al., 1991).

Atlantis Bank itself presents a nearly flat summit, with over 25 km^2 lying between depths of 800 and 690 m (Dick et al., 1991a). The Bank was produced by wave-erosion at sea level (Robinson, Von Herzen, et al., 1989) and is partly capped by thin, shallow-water limestone containing large molluscs, snails, echinoids, and varieties of coral. The limestone embeds boulders of gabbro that were cast down from sea cliffs and rounded in the surf (MacLeod et al., 1998; Dick et al., 1999a). The rest of the surface, mainly in the center of the bank, but including a westward extension around Hole 735B, is a somewhat rougher gabbro exposure, the wave-beveled remnant of sea stacks, that is now swept clear of sediments by mid-water currents. Within the unsedimented gabbros, networks of veins and other structure have been discerned using near-bottom video equipment (MacLeod et al., 1998; Leg 176 Scientific Party, 1999).

Atlantis Bank probably was uplifted to sea level within about two million years of crystallization of gabbros beneath the rift valley floor, to a location adjacent to, and immediately south of, a very deep nodal basin like the one currently located at the present ridge-transform intersection (Dick et al., 1991a). Presently, the summit peak of the transverse ridge nearest the nodal basin rises to less than 1900 m. A similar but much smaller feature named Anna de Koenigh Seamount reaches to less than 200 m adjacent to, and immediately north of, a nodal basin at the junction of the transform portion of DuToit Fracture Zone and the Southwest Indian Ridge (Fisher et al., 1986). Rounded gabbro boulders in a dredge haul near the top of the seamount demonstrate that the summit there was at wave base when sea level was lower earlier in the Pleistocene. Assuming a similar origin for Atlantis Bank, wave truncation and formation of the thin limestone carapace over a portion of the summit, then total submergence, were followed by gradual subsidence to the present depth of around 700 m.

Although we did not reach either altered or fresh peridotites at Hole 735B, dive samples obtained during a post-drilling submersible survey (Dick et al., 1999a) show that the bottom of Hole 735B, at 1508 mbsf, is approximately at the level of talcose serpentinized peridotites obtained on the western slope of Atlantis Bank, some 3 km to the west of the drill site. Serpentinized peridotites were obtained at still shallower depths on the eastern slope of Atlantis Bank and even on the southern end of its flat summit. If the gabbro-peridotite contact is planar, and simply dips to the north, as does all of the deformational

structure within the cores of Hole 735B, then the base of the gabbroic sequence at most appears to be 200–600 m below the bottom of the hole. A similar reconstruction of the structure suggests that the top of Hole 735B is about 500 m below the base of any kind of dike sequence. Hole 735B thus comprises about 60–70% of the likely gabbroic section at this location. Fluid-inclusion studies on samples from near the top of the hole (Vanko and Stakes, 1991) suggest that about 2 km of overburden, chiefly basalts and dikes, was removed by tectonic processes and erosion. A rough estimate for the original thickness of magmatic crust at Hole 735B is thus about 4 km, approximately the same as that suggested by petrologic inference (Muller et al., 1997). Depth to seismic Moho at the site, however, is estimated to be 5 km below the seafloor (Minshull and White, 1996), some 3 km deeper than the probable thickness of gabbros. Therefore, partially serpentinized peridotite almost certainly is present between the gabbros of Hole 735B and Moho.

To summarize, although our concept of the spreading process is usually that of accretion of igneous material at the ridge axis within the rift valley, on the Southwest Indian Ridge a general additional attribute of the ocean crust must be acknowledged. This is that a great deal of the crust in this region has a profound topographic corrugation resulting from the close spacing of transform faults, and the presence of tectonically uplifted, high transverse ridges in between. In regional bathymetry (Fisher and Goodwillie, 1997) and in the geoid (Rommeveaux-Jestin et al., 1997), fracture zones and transverse ridges dominate the Southwest Indian Ridge. Mid-segment crust is in the minority. The rocks drilled at Hole 735B thus were exposed by general processes and are *not* atypical of this or any other rifted, slowly-spreading ridge. Of most importance, accretion acted while the rocks were being deformed and sheared beneath the rift-valley floor. Neither magmatism nor formation of cumulates are possible to separate from the tectonic processes that led to formation of the profound topography of the Southwest Indian Ridge.

3. Lithostratigraphy

General results of Leg 176 and the protocols for descriptions of rocks and thin sections are summarized elsewhere (Dick et al., 1999a; Dick et al., 2000; Robinson et al., (in press)). The following is based chiefly on shipboard descriptions and XRF chemical analyses (Robinson, Von Herzen et al., 1989; Dick, Natland, Miller et al. 1999).

In outline, the section drilled over two legs consists of five main masses of relatively primitive olivine gabbro and troctolite, each from 200 to 450 m thick, and each with its own internal chemical and petrological coherence (Fig. 2A). Overall, each of these plutonic masses is composed of many smaller gabbroic bodies, which separately probably represent small intrusive masses (or cooling units), typically $\leq$1 m in thickness, that penetrated fairly cold rock, in which case contacts are sharp, or more usually crystal mushes, in which cases contacts are diffuse or sutured. Almost all are oblique to the long direction of the core. During Leg 176, 457 such small igneous bodies, termed 'intervals', were described, adding to the 495 described during Leg 118 (Dick et al., 1991b). A running average of the proportion of different igneous lithologies represented by these intervals and taken 20 intervals at a time is plotted against depth in Fig. 2B. This shows that the upper, middle, and lower 500-m portions of Hole 735B are each distinct, and in no way replicate each other. There are numerous small crosscutting intervals of olivine gabbro, microgabbro, and troctolite within the larger plutonic masses. In the deepest pluton reached, a number of these are narrow and nearly vertical pipe-like bodies that may represent feeder channels for melts that migrated upward through crystal mushes. Each of the larger, composite plutonic bodies nevertheless has a preponderance of more differentiated gabbro and gabbronorite toward its top, and the most primitive and magnesian rocks, toward its base. Each therefore probably represents a substantial pulse of magma, albeit injected one small bit at a time, but which in toto added significantly to the thickness of this block of ocean crust. Each pluton also individually experienced cooling and a great deal of internal magmatic differentiation even as it was being injected.

There are varieties of grain-size, modal, pegmatitic, and deformational layering in the gabbros of Hole 735B. These are of unknown lateral extent, and deformational layering is most common. The thick, intensely layered sequences that occur in many

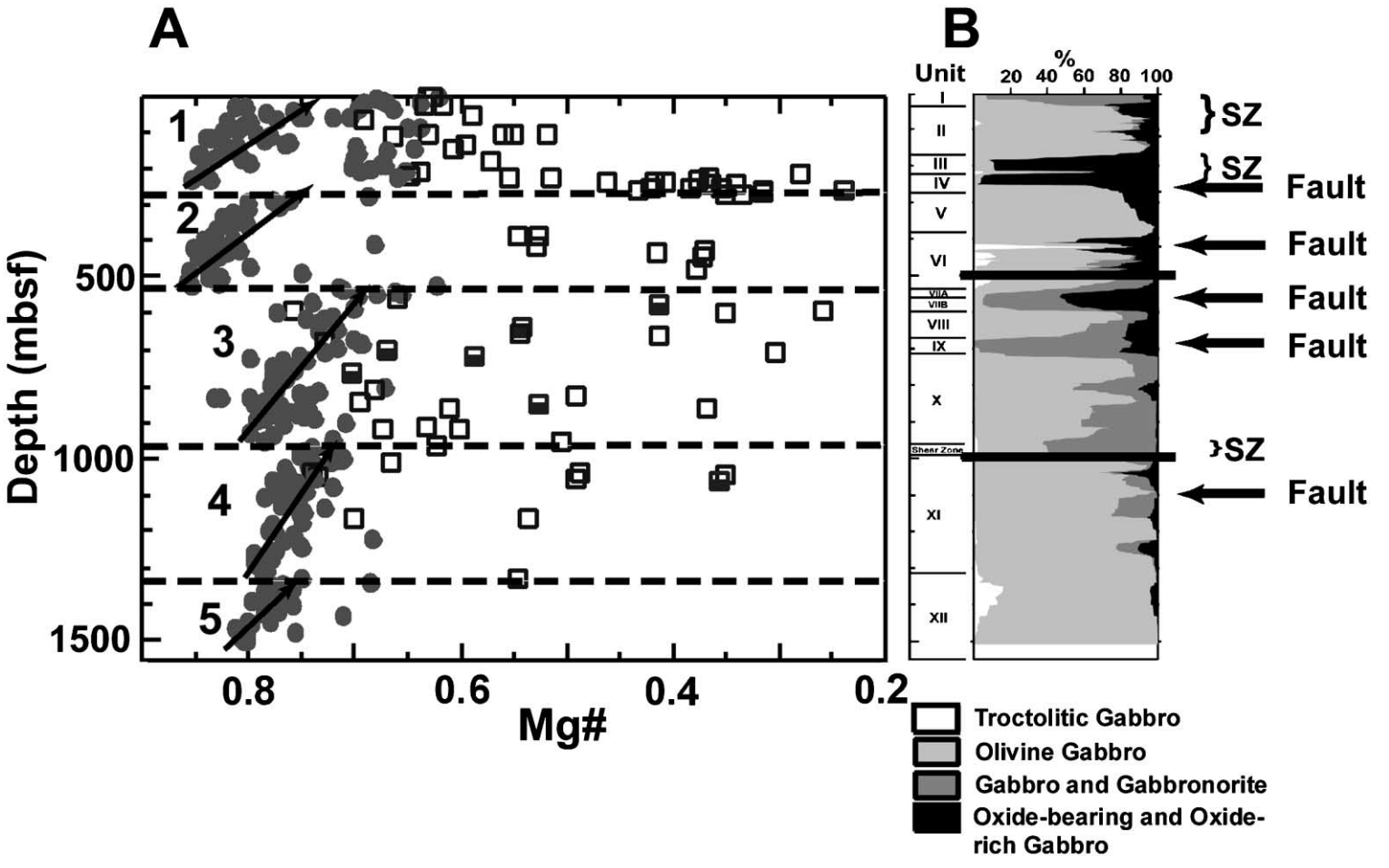

Fig. 2. Chemical- and lithostratigraphic summary of Hole 735B. Data are from Robinson et al. (1989), Dick et al. (1999), and J. Hertogen (unpublished). (A) Mg# vs. depth. Mg# = Mg/([Mg + Fe^{2+}], assuming that $Fe^{2+}/[Fe^{2+} + Fe^{3+}] = 0.86$. Filled circles = samples with TiO_2 0.7%, mainly troctolites and olivine gabbros. Open squares = samples with $TiO_2 > 0.7\%$, mainly oxide-bearing gabbro and gabbronorite and oxide-rich gabbros. Half-filled squares = samples with $SiO_2 > 56\%$, including ferrodiorites, trondhjemites, and one granite. Dashed lines at bases of major breaks in compositional trends of troctolites and olivine gabbros define five principal plutonic masses within the drilled section, each becoming more differentiated (proportionally iron-rich) upward, as indicated by the diagonal arrows. All other samples represent narrow, cross-cutting facies each typically 5–15 cm thick. (B) Simplified summary lithostratigraphy giving (left to right) the main lithologic units defined during Legs 118 and 176, proportions (%) of intervals of principal lithofacies (indicated in the key) constructed using a rolling average at 20 m intervals, and structure. Note that the the oxide-bearing and oxide-rich gabbros (black) correspond to the open squares in A. Horizontal lines are drawn across the lithofacies summary at 500 m intervals (see text for discussion). Under structure, SZ = shear zone, F = fault.

layered intrusions and the lower portions of some ophiolites, are not present. Less than 2% of the rocks have modal or graded layering, of the type that might result from either mechanical sorting of minerals separating from moving magmas or from compositional changes in magma during deposition of the minerals. Such occurrences are usually restricted to one or two layers. The best example of repetitive layering is an interval of 9 m (837–846 mbsf) within which there are 34 normally graded layers, each with plagioclase proportions and grain sizes increasing downward, and ranging from 6–22 cm in thickness. The mechanism of layering in this interval has not been determined.

Although the boundaries of each of the larger plutonic masses are fairly well defined, the relationships of one to another are neither simple nor consistent. The uppermost one is separated from the one underneath by about 70 m of iron-and titanium-rich oxide gabbro, within which there are numerous narrow but intense zones of shear. A small and abrupt deformational offset separates the lower two plutons, although the extent of the offset is probably not great. There is a zone of brittle faulting near the contact between the second and third masses, but it is not at the contact. Instead, the contact, which is actually distributed over a zone of several tens of meters, is marked by a series of crosscutting gabbros and olivine gabbros, and appears overall to be intrusive in character. The occurrence of composite intrusions, with large-scale repetitions of crystallization sequences, indicates that this portion of the Southwest Indian Ridge was supplied magma in several pulses, rather than by steady and persistent flow.

Small seams of oxide-bearing and oxide-rich gabbro, each only a few to tens of centimeters thick, cross the core in many places. There are 647 such seams in the lower 1004 m of the hole, as established by routine measurement of magnetic susceptibility using the shipboard multisensor track (MST; Fig. 3). Measurements were made at 4 cm intervals along the entire 867 m of core recovered in this interval during Leg 176. Magnetic susceptibility is sensitive to the quantity of fairly coarse-grained magnetite in the rocks, particularly that present in coarse aggregates of the magmatic iron–titanium oxides, ilmenite and magnetite (Fig. 3B). There is a good correlation, for example, between magnetic susceptibility and the quantity of TiO_2 measured in individual samples. The largest concentration of rock with high magnetic susceptibility, however, is the zone of nearly pure oxide gabbro cored between 200 and 270 mbsf during Leg 118 (Fig. 3A), for which susceptibility was determined by downhole logging (Pariso et al., 1991) and measurement on discrete samples (Kikawa and Pariso, 1991). Individual samples in this portion of the core typically contain 5–15% of ilmenite and magnetite. In rare cases, the proportion of these oxide minerals exceeds 30% (Bloomer et al., 1991). Below 504 mbsf, in the rocks described during Leg 176, many of the hundreds of narrow oxide-rich seams (Fig. 3C) are associated with veins of siliceous diorite, trondhjemite, and granodiorite (Figs. 3D and 4); a total of 203 of these were annotated in the core descriptions. Below 200 mbsf, the oxide-rich seams diminish sporadically, but nevertheless quite steadily, down the hole (Fig. 3B), as does the incidence of felsic veins (Fig. 3E), the total of both decreasing to less

Fig. 3. Magnetic susceptibility at Hole 735B. (A) As measured using the downhole magnetic susceptibility log during Leg 118 (Pariso et al., 1991). Major lithologic units and principal zones of deformation are as in Robinson et al. (1989). Chemical zones are from Natland et al. (1991). Note that susceptibility is given in cgs units and that depth is given in meters below the rig floor. (B) Thickness of intervals of oxide gabbro, plotted as a rolling 20 m average, compared to the number of measurements of magnetic susceptibility above a threshold given by the vertical line in C. For the Leg 118 portion of the core, magnetic susceptibility is plotted as a 50 m rolling average of measurements in Kikawa and Pariso (1991). For the Leg 176 portion of the core, it is plotted as a 20 m rolling average based on measurements using the multi-sensor track (MST). (C) Magnetic susceptibility in MU as measured at 4 cm intervals by MST on whole-round core during Leg 176. Susceptibility is given in machine units MU, for which a geometric factor (0.67) must be used to convert to SI units. (D) Blow-up of the interval for one core showing magnetic susceptibility peaks, and their correlation with identified and numbered lithologic intervals (LI), and the occurrences of numbered felsic veins (FV) in the core, as noted in spreadsheets. There is one additional notation in the vein comments spreadsheet. The lines to the right indicate the bases only of three narrow lithologic intervals, as indicated by number. Two of these are oxide gabbros, and the third is a sheared olivine gabbro that contains a felsic vein and some oxides. OxG = oxide gabbro. OG = olivine gabbro. Intervening longer intervals are of olivine gabbros. Two susceptibility spikes annoted with question marks were not noted in any descriptive log. (E) Volume% of felsic veins per 10 m interval vs. depth. (F) Fabric intensity, indicative of crystal–plastic deformation vs. depth. See text for a description of the scale.

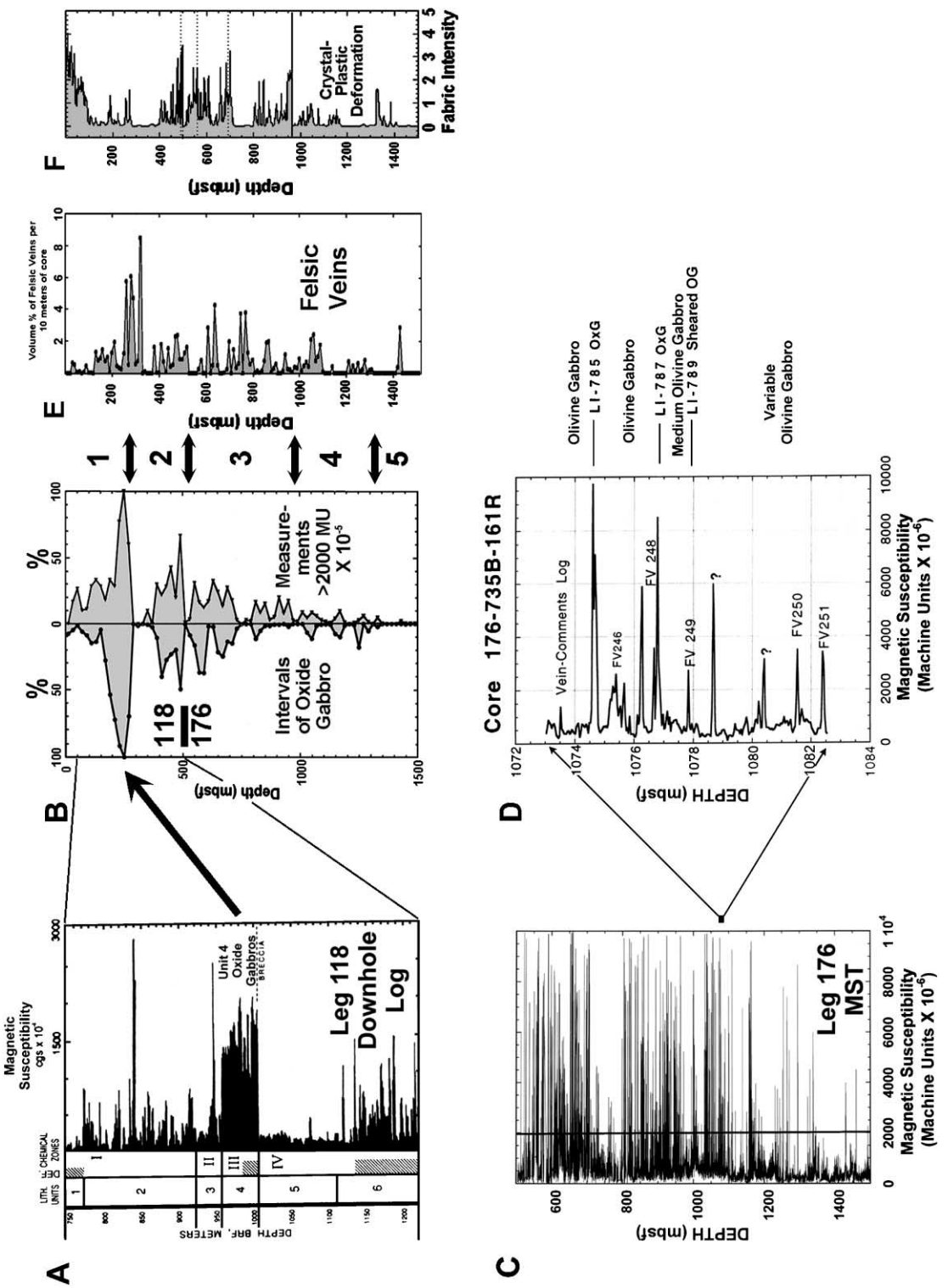
A
Magnetic Susceptibility cgs x 10⁻³
Leg 118 Downhole Log
Unit 4 Oxide Gabbros
BRECCIA
LITH. UNITS
CHEMICAL ZONES
DEPTH BRF. METERS
B
Depth (mbsf)
118
176
Intervals of Oxide Gabbro
Measure-ments >2000 MU X 10⁻³
%
1
2
3
4
5
E
Volume % of Felsic Veins per 10 meters of core
Felsic Veins
Depth (mbsf)
F
Crystal-Plastic Deformation
Fabric Intensity
C
Leg 176 MST
DEPTH (mbsf)
Magnetic Susceptibility (Machine Units X 10⁻⁶)
D
Core 176-735B-161R
Vein-Comments Log
FV246
FV 248
FV 249
FV250
FV251
Olivine Gabbro
LI-785 OxG
Olivine Gabbro
LI-787 OxG
Medium Olivine Gabbro
LI-789 Sheared OG
Variable Olivine Gabbro
DEPTH (mbsf)
Magnetic Susceptibility (Machine Units X 10⁻⁶)

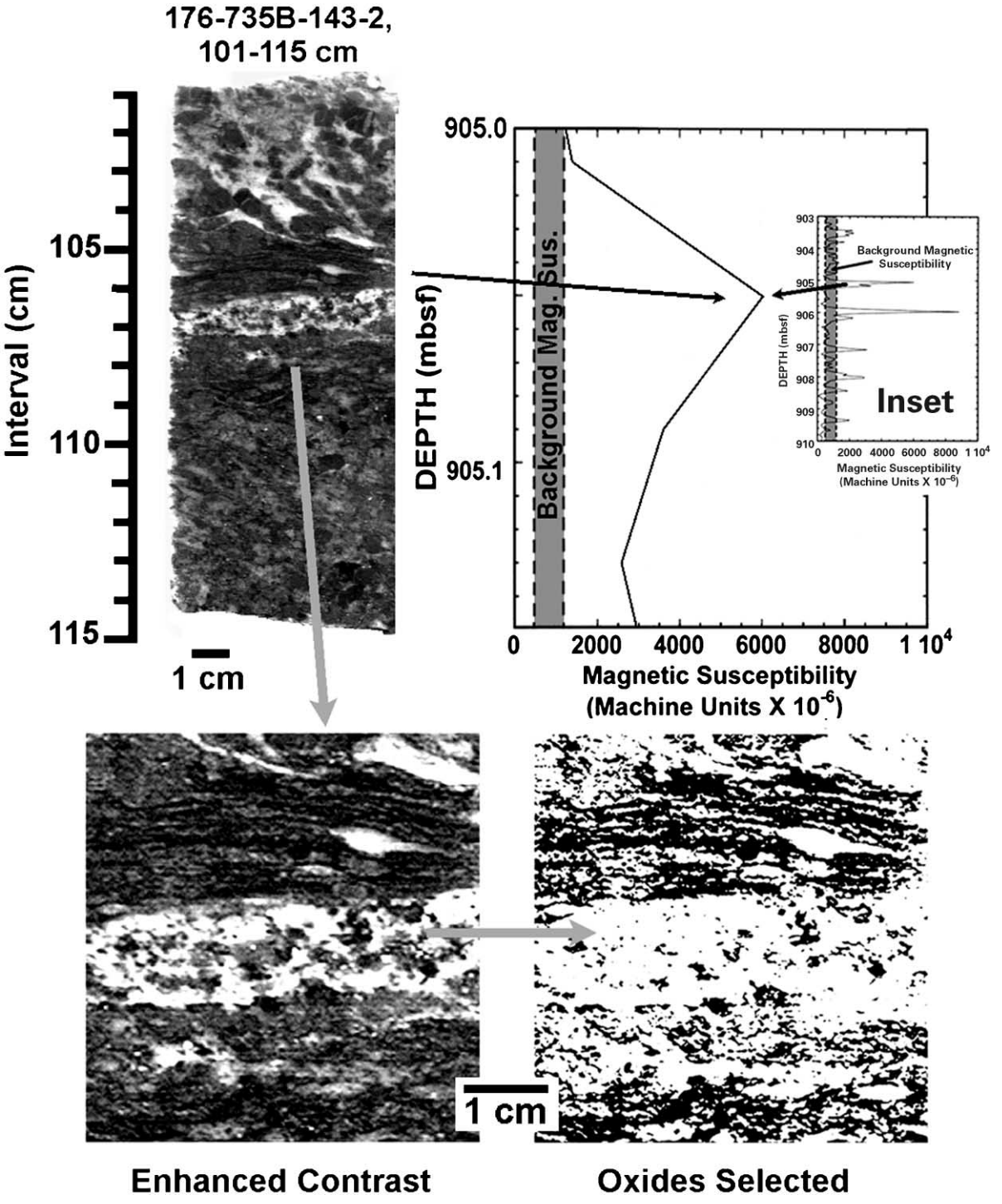
176-735B-143-2,
101-115 cm
Interval (cm)
105
110
115
1 cm
905.0
905.1
DEPTH (mbsf)
Background Mag. Sus.
0
2000
4000
6000
8000
1 10^4
Magnetic Susceptibility
(Machine Units X 10^-6)
Background Magnetic Susceptibility
Inset
903
904
905
906
907
908
909
910
DEPTH (mbsf)
0 2000 4000 6000 8000 1 10^4
Magnetic Susceptibility
(Machine Units X 10^-6)
1 cm
Enhanced Contrast
Oxides Selected

than 1% of the recovered core in the lower 300 m of the hole.

The proportion and distribution of oxide-rich intervals is different in each of the five plutons (Fig. 3B). In the upper two, they are concentrated toward the bases of the plutons; in the next lower they are concentrated toward the top. In the lowest two, they are scattered. The felsic veins also show no consistent relationship to the boundaries of the five plutons and, although their general distribution is similar to that of the oxide seams, the pattern is not identical. Some simply vein olivine gabbro. The patterns of both oxide seams and felsic veins consequently appear to be superimposed structurally on the underlying framework of olivine gabbros and gabbros. They are not, for example, concentrated in intermediate 'sandwich' horizons in any of the five plutons, nor near their tops, nor are they altogether absent even near the bottom of the hole. The full course of differentiation is represented to some degree at all levels, but the physical distribution of the most differentiated rocks is independent of the underlying basic pattern of differentiation represented by the matrix troctolites and olivine gabbros. This is not the pattern of typical layered intrusions or of well-studied ophiolites such as Troodos, Oman, or Bay of Islands.

4. Structure

Gabbros recovered during Leg 176, like those drilled during Leg 118, display numerous magmatic, crystal–plastic, and brittle deformation features. The structural element of most significance to processes of magmatic differentiation is intensity of crystal–plastic deformation, which is a measure of the extent of foliation of the rocks on a scale of 0–5 (Dick, Natland, Miller et al., 1999). Fabric intensities 2–5 correspond to strongly foliated (usually gneissic), porphyroclastic, mylonitic and ultramylonitic fabrics, in that order. Such rocks comprise about 20% of the total core described during both legs. Idiomorphic relations in thin section (Natland et al., 1991) and the compositions of coexisting amphibole and plagioclase (Stakes et al., 1991) indicate that these fabrics were produced during a combination of late magmatic and granulite-facies metamorphic conditions, generally above about 700°C. Below the thick interval of oxide gabbros at about 270 mbsf, here is a strong general correspondence between variation of fabric intensity and the abundance of oxide minerals, as determined by both lithologic observations and magnetic susceptibility (Fig. 3B and F). This comprises some 82% of the hole down to its base. That is, through most of the core there is a strong tendency for seams of oxide gabbro to be associated with zones of strong deformation, although this does not mean that oxide gabbros are always or even the only foliated rocks, nor that they are the most foliated rocks in a given strongly deformed interval.

Above this, trends are different. The massive oxide gabbros from 200–270 mbsf are only sporadically gneissic and porphyroclastic, and the most deformed rocks are at the very top of the hole, where oxide gabbros are scant. We tentatively relate the intensely deformed rocks at the top of the hole to proximity to the fault surface along which the summit of Atlantis Bank was originally exposed. That surface was originally corrugated (Dick et al., 1999a,b), as it is on the summits of core complexes or 'mega-mullions' adjacent to transform faults along the Mid-Atlantic Ridge (Cann et al., 1997; Tucholke et al., 1998). Erosion at wave base has cut into this surface, but the rocks in the upper 100 m also show fairly extensive oxidative alteration and an upward spike in both strontium and oxygen isotopes (Stakes et al., 1991; Kempton et al., 1991; Hart et al., 1999), unlike anything further down. Reaction between the rocks and cool, shallow oxygenated seawater or perhaps even a fresh water lens comprising the water table beneath the uplifted island may be the cause of this alteration.

Scarcity of pronounced foliation in the massive

Fig. 4. Scanned image of an example of the association of a felsic vein (white) with oxide-rich gabbro at about 905 mbsf in Hole 735B (upper left), linked to multi-sensor track (MST) measurements of magnetic susceptibility at 4 cm intervals on the unsplit core (upper right). The magnetic susceptibility inset shows the individual susceptibility peak among several others in a 7 m section of core. Over 600 similar peaks were measured altogether in the 1004 m of core drilled during Leg 176, almost all of them indicating very local high proportions of magmatic oxides in the core. The lower panels focus on the nearly horizontal felsic vein, and show, by means of successive enhanced-contrast selection of the dark oxide minerals, the association of coarse ilmenite and magnetite with the vein, and that rock near the vein is strongly foliated.

oxide gabbros from 200–270 mbsf does not mean that these rocks are 'undeformed'. There are in fact several cycles, some 10–20 m thick, of increasing deformation downward in this interval through the sequence: gneissic, porphyroclastic, and mylonitic, with one narrow oxide-rich ultramylonite (Cannat, 1991) so dark and compact that was at first confused for a thin basalt dike. The porphyroclastic and mylontic rocks do not have a strong preferential orientation of minerals, but instead are sequentially more pulverized rock. Only the gneissic rocks are foliated. Ilmenite and magnetite are locally so abundant that some of the undeformed rocks are essentially breccias of deformed fragments 'cemented' by large proportions of these minerals (Bloomer et al., 1991). In these rocks, the oxide minerals precipitated from late-stage melts *after* strong deformation of host rocks, and the late precipitating oxide minerals were never subsequently strongly sheared (Natland et al., 1991).

In the lower half of the hole, intervals up to 150 m thick are comparatively free of shear deformation (Fig. 3E) and are either texturally isotropic, or contain weak to moderate magmatic foliation. A weak parallel fabric that may record the transition from magmatic to crystal–plastic deformation commonly overprints magmatic foliation. Locally, however, foliation is fairly well developed, and in one interval of about 200 m thickness, there are a number of high-temperature reverse shear zones. Many of the deformed rocks record a continuum between crystal–plastic and brittle behavior that corresponded to a shift in conditions of hydrothermal alteration from amphibolite to greenschist facies. There are also some narrow zones of intense cataclasis, and several fault zones were identified (Fig. 2B). Two of these were detected by a vertical seismic profile (VSP) experiment during Leg 118 (Swift et al., 1991), before the rocks were reached by drilling during Leg 176.

5. Metamorphism

The metamorphism and alteration in the rocks of Hole 735B can be pictured as a continuum, but with the most pronounced effects being recorded in two sorts of rocks: (1) A high-temperature sequence, from granulite to amphibolite facies, formed in a dynamic environment with only minor greenschist mineralization, as the rocks cooled from magmatic temperatures through the subsolidus; and (2) a lower-temperature sequence, related to different sets of fractures, formed in veins that are usually oblique or orthogonal to prior foliation, and in adjacent rock.

During the first stage, some of the most striking zones of crystal–plastic deformation formed under granulite-facies metamorphic conditions (>800–1000°C), in the presence of little or no melt. This should be viewed as a continuation of the deformation that began when the rocks were still partly molten. Then a fair amount of static replacement of primary silicates, chiefly by varieties of amphibole, took place (e.g. Stakes et al., 1991; Robinson et al., (in press)). Late magmatic and hydrothermal fluids locally transformed the rock in two shear zones in the upper 600 m to amphibole and more sodic plagioclase, and in both zones there are veins of plagioclase, amphibole, and diopside in various combinations. Overall, however, static high-temperature alteration was patchy rather than pervasive, and most of it is concentrated toward the top of the hole. Extensive intervals >300 m thick have less than 10% background alteration. Most rocks are extremely fresh.

The low-temperature alteration stage is most obvious below 500 mbsf, and is represented by formation of abundant late smectite–chlorite, carbonate, and zeolite–prehnite veins, locally with iron oxyhydroxides. Smectite–chlorite, calcite, and iron oxyhydroxides are particularly prevalent in a zone of intense alteration between 500–600 mbsf. Deeper in the hole, there are locally abundant fractures lined with smectite–chlorite. These are associated with sulfides, indicating formation under non-oxidative conditions at fairly low temperature. Whereas most veins near the top of the hole are inclined, these are more usually vertical. The only sequence with pervasive, as opposed to patchy, oxidative alteration, in which olivine, for example, is consistently replaced by clays and iron oxyhydroxides, is the uppermost 100 m of core, as discussed previously.

The first, high-temperature, stage of metamorphism occurred beneath the floor of the rift valley, beginning while melt was still present in the rocks, and continuing while the rocks were still very hot and susceptible to crystal–plastic deformation. Amphibolite-facies metamorphism was more static, but was superimposed on both deformed and undeformed rock

adjacent to generally inclined fractures while the rocks were still quite hot. Fracture porosity at this point was highest in the upper third of the section. The rocks continued to cool, but did not react extensively with formation fluids through greenschist conditions, presumably because of low formation porosity and permeability. Exposure and uplift to the summit of the transverse ridge increased permeability by producing a new set of fractures, predominantly horizontal and vertical, near the bottom of the hole, and some faults along which now cooler fluids could flow, producing the low-temperature metamorphic assemblages.

6. Rock magnetics

Rock magnetic measurements show that the entire body of rock cored during Legs 118 and 176 has a consistent average stable inclination of 71.4°, and no significant downhole variation (Kikawa and Pariso, 1991; Dick, Natland, Miller et al., 1999). The rocks were tilted by about 19°, but have a very stable remnant magnetization and often very sharp blocking temperatures, suggesting relatively rapid acquisition of thermoremanence during cooling. This cooling took place while the rocks were beneath the rift valley and relatively shortly after they crystallized. The mineral producing the stable magnetization is secondary magnetite that formed in conjunction with hydrothermal alteration of the rocks to assemblages including high-temperature amphibole. This followed all of the deformation that produced foliation, but before the rocks were exhumed from beneath the rift valley. The entire body of rock remained essentially intact during its uplift to the summit of Atlantis Bank, only it rotated somewhat to the south. Analysis of structures re-oriented magnetically indicates that the dominant foliation dips preferentially toward the rift axis to the north.

Downhole variations recorded in stable inclinations and magnetizations in basalts drilled elsewhere on slowly spreading ridges, and their structural complexities, are evidently sufficient to confound the magnetic signature of the uppermost extrusive portion of the ocean crust, making it an inadequate source layer for magnetic anomalies (Flower and Robinson, 1979; Hall, 1979). A gabbroic layer as thick as our drilled section is sufficient to account for the marine magnetic anomaly near Hole 735B on Atlantis Bank (Dick et al., 2000). In fact, the gabbroic layer drilled at Hole 735B represents the *only* portion of ocean crust drilled thus far that has provided a magnetic signature consistent enough to produce a magnetic anomaly. Gabbros in general thus are a potential source for marine magnetic anomalies worldwide, beneath the more complicated basalts.

7. Physical properties and relationship to seismic structure

Several hundred minicores were measured for densities and compressional velocities during Legs 118 and 176. Oxide gabbros are denser than olivine gabbros, reaching 3.2 gm/cm^3, compared with an average of all lithologies of 2.98 ± 0.10 gm/cm^3. The densities are appropriate for rocks attributed to Seismic Layer 3 in the ocean crust. There is no relationship between minicore densities or velocities and zones of low density, porosity, and permeability detected by downhole logs, not even in samples obtained from cores that penetrated two reflectors, one at 560 mbsf, the other at 760–825 mbsf, measured during the Leg 118 vertical seismic experiment (Swift et al., 1991). The reflectors do not correspond to boundaries between any of the several gabbro plutons in the core nor the mass of oxide gabbros between 200–270 mbsf. The reflectors thus are not the result of the intrinsic physical properties of the gabbros themselves, either the development of a strong preferred mineral fabric or variations in density. Instead, they correspond to faults and fractures, for which we found evidence in the cores in the form of reduced recovery, substantial hydrothermal alteration, and fractures lined with slickensided minerals. However, offsets and rotations along the faults do not significantly disrupt or offset either the lithostratigraphy or the magnetic stratigraphy. In these respects, the drilled section is essentially the same as when it was beneath the floor of the rift valley, and still fairly hot, above Curie temperatures, just before its exposure and uplift. The rocks only lightly record the entire subsequent history of uplift to the summit of the transverse ridge, erosion, and subsidence.

8. Summary of principal variations with depth

In what way does this section change with depth? The five-stacked plutons generally overlap in bulk composition, and presumably therefore in cryptic variation of mineral compositions. There is thus no indication that rocks overall are more primitive with depth, as in well-studied ophiolites such as Oman, Troodos, and Bay of Islands. Indeed, the most primitive rocks, spinel-bearing troctolites, are far from the bottom of the hole, at the base of the second pluton down. There may be still deeper plutons, no more differentiated than the ones already cored, between the bottom of the hole and serpentinized peridotite.

There are some changes with depth however, in features of the core that were superimposed on the basic structure of nested plutons, as follows: (1) beneath the major zone of oxide gabbros between 200–270 mbsf, there are hundreds of seams of oxide gabbros, but these diminish to nearly nil in the lower 300 m of the hole; (2) there are also fewer felsic veins with depth; (3) there is less crystal–plastic deformation near the bottom of the hole; (4) there are faint indications that modal and grain-size layering is better developed near the bottom of the hole; (5) there are some near-vertical intrusions of primitive olivine microgabbro deep in the hole, not present elsewhere; (6) the orientation of veins shifts from predominantly inclined, to predominantly horizontal and vertical, with depth; and (7) the minerals in the horizontal and vertical veins are predominantly smectite/chlorite and zeolite rather than the amphibole, plagioclase, and diopside common in veins further up. If, as we believe, the deeper, low-temperature veins resulted from dilatancy fracturing during cooling of the uplifted block after unroofing, and they are subtracted from the total vein assemblage, then the remaining high-temperature veins — those that formed deep beneath the rift valley — are strongly concentrated in the upper third of the hole. High-temperature fracturing and mineralization did not so strongly affect deeper rocks. Penetration of fluids at the ridge axis therefore diminished with depth, and most of it occurred when inclined systems of presumed detachment faults penetrated the crystallizing body of rock, or shortly thereafter.

These several patterns indicate that the drill string indeed reached fairly deep into the lower ocean crust, where intrusion, differentiation, melt flow, and deformation occurred at higher temperatures, on average, and with less extreme fluctuations, than near the top of the hole. The gabbros of Hole 735B consequently present a variety of complicated and interrelated igneous, structural, metamorphic, magnetic, and physical attributes from which a general picture of the formation of ocean crust at this very slowly spreading ridge can be constructed. The greatest complication is that the most intense deformation was closely tied to magmatism prior to hydrothermal metamorphism, magnetization, and uplift of the rocks from beneath the rift valley. This will be the main issue addressed in the following discussion.

9. Crystallization of cumulates

This section describes the distinctive array of cumulus processes exhibited by gabbros of Hole 735B. Evidence against the presence of any substantial magma body in the history of these gabbros has already been summarized. That the rocks do not resemble those of the large layered intrusions, which constitute the principal materials from which the theory of cumulates has been constructed, is evident from the basic underlying stratigraphy of small, nested plutons, the dearth of modal and grain-size

Fig. 5. Comparison of aspects of the bulk composition and mineralogy of gabbros of Hole 735B and basalts from the Indian Ocean. (A) *Mg* (= cationic MgO/[MgO + FeO]; all iron as Fe^{2+}) vs. *Ca* (= cationic CaO/[CaO + NaO]), calculated from shipboard XRF analyses. Gray symbols are basalts, black rght-pointing triangles are gabbros. See text for additional explanation. (B) An vs. Fo (mole%) of intergrown olivine and plagioclase in gabbros of Hole 735B and Indian Ocean basalts. Gabbros are small dots. Basalts are larger symbols. Open squares are from a type 1 basalt, also indicated in A, from DSDP 212; Large filled dots are from type 2 basalts of the Central and Southeast Indian Ridges; the filled diamond is from a type 2 basalt from the Southwest Indian Ridge. The gray square is from a type 3 basalt between Atlantis II Fracture Zone and the triple junction. The histograms represent all analyzed olivines and plagioclases, of which only a fraction are intergrown in glomerocrysts. Basalt compositions, mainly of glasses, are from the literature and J. Natland (unpublished data). Hole 735B mineral data are from Ozawa et al. (1991), Hébert et al. (1991), Stakes et al. (1991) and Natland et al. (1991). Phenocryst data are mainly from data files of J. Natland (unpublished), and also sources in the literature.

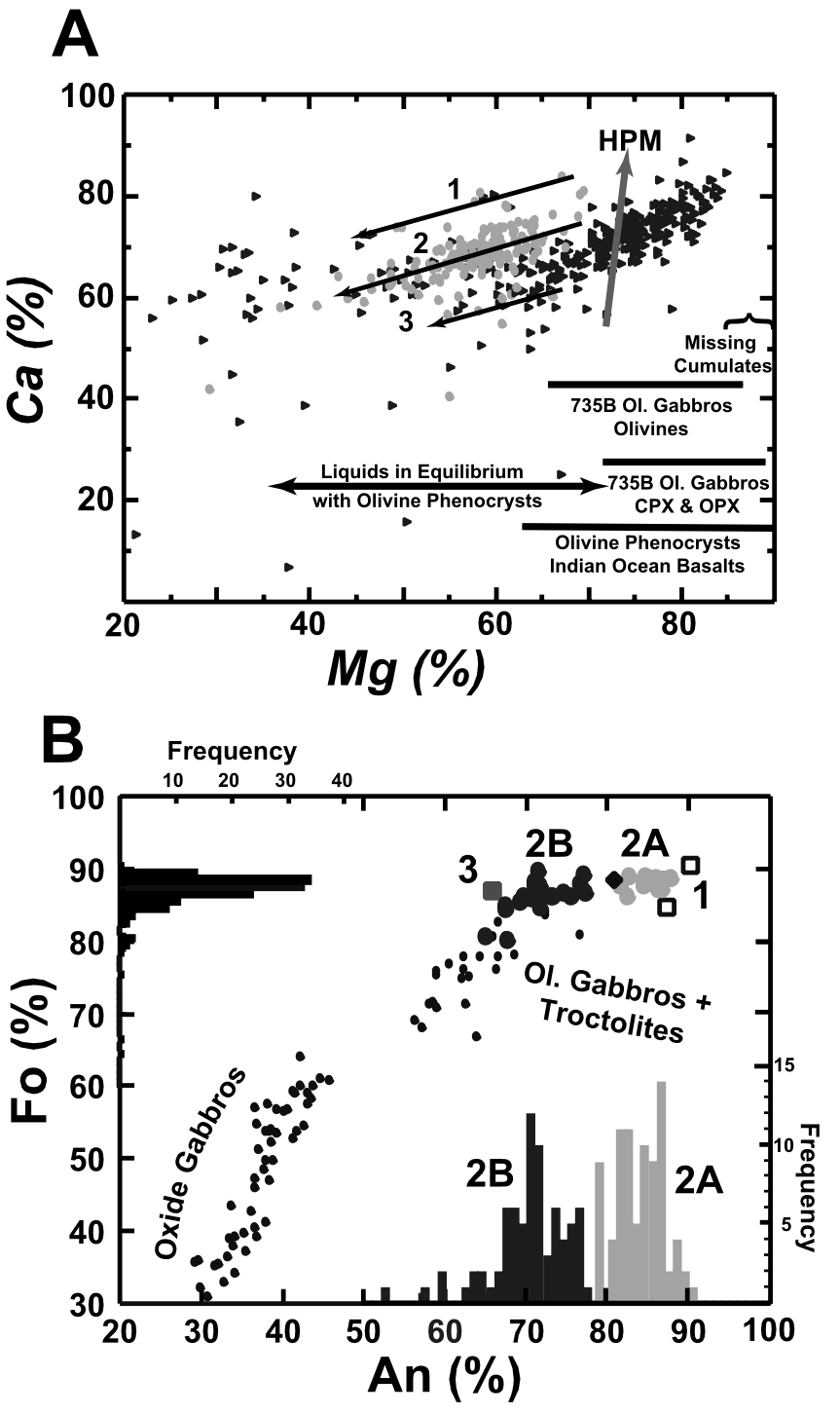
A
Ca (%)
Mg (%)
HPM
1
2
3
Missing
Cumulates
735B Ol. Gabbros
Olivines
Liquids in Equilibrium
with Olivine Phenocrysts
735B Ol. Gabbros
CPX & OPX
Olivine Phenocrysts
Indian Ocean Basalts
B
Frequency
Fo (%)
An (%)
2B
2A
3
1
Ol. Gabbros +
Troctolites
Oxide Gabbros
Frequency

layering, and the independent patterns of cross-cutting oxide seams and felsic veins, which provide hundreds of sharp lithologic truncations and both small- and large-scale fluctuations in the patterns of modal and cryptic mineralogical variation in the cores.

9.1. Hole 735B gabbros as cumulates

Igneous petrologists of both Legs 118 and 176 considered almost all of the rocks of Hole 735B to be cumulates because none of the gabbros have the compositions of basaltic liquids, and are instead the products of *fractional crystallization* of those liquids (Irvine, 1982). Fig. 5A compares aspects of the composition of gabbros of Hole 735B with data for all Indian Ocean basalts collected prior to Leg 176. These are mainly glasses. The ones obtained near Hole 735B are fairly typical depleted abyssal tholeiites. Like all basalts of rifted, slowly spreading ridges, these are only moderately differentiated, with none achieving the extent of iron-enrichment so commonly observed at fast-spreading ridges (Dick et al., 1991a; Natland et al., 1991).

In Fig. 5A, *Mg* expresses extent of differentiation of basalts, whereas *Ca* is an indicator both of extent of differentiation and parental characteristics. Thus there is a fair span in Ca even at high *Mg*. Parental *Ca*, say at $Mg = 70$, therefore can be considered somewhat analogous to the parameter Na_8 of Klein and Langmuir (1987), which depends on the extent of partial melting. The near-vertical arrow on the right indicates a general trend of increasing extent of partial melting (toward higher *Ca*, therefore lower Na_8) for hypothetical primitive MORB liquids (Kinzler and Grove, 1993). The inclined arrows to the left give the general trend of low-pressure differentiation of three different basalt types in the Indian Ocean, these having low, intermediate, and high Na_8, with the arrow labeled 2 being appropriate to basalts from most of the Indian Ocean, including Atlantis II Fracture Zone.

The largest cluster of data points for gabbros is a curving trend on the right side of the diagram, comprising olivine gabbros and troctolites. It curves concentrically to the field for basalts, and overlaps it very little. *Mg* in many of these gabbros is higher than in hypothetical primitive liquids. The higher *Mg* derives from the compositions of cumulus olivine and pyroxenes, indicated by ranges shown at the lower right (from Hébert et al., 1991; Ozawa et al., 1991; Bloomer et al., 1991; Natland et al., 1991). Also shown is the range of Fo contents for olivine phenocrysts (J. Natland, unpublished data), and a double-arrowed range for liquids in equilibrium with those phenocrysts ($K_D = 0.28$; Hébert et al., 1991, based on the formulation of Roeder and Emslie, 1970). The calculated liquids match the *Mg* range of Indian Ocean basalts that are, once again, mainly glasses.

Fig. 5B provides a more detailed comparison of the compositions of coexisting olivine and plagioclase in Hole 735B gabbros and the compositions of the same minerals in Indian Ocean basalts, whether present as individual phenocrysts (histograms) or intergrown pairs of these minerals in glomerocrysts (plotted data points). Numbers on the diagram correspond to basalt types 1, 2 and 3 of Fig. 10A. Whereas there is overlap between gabbro olivine compositions and those of individual olivine phenocrysts given by the histogram on the left, only a portion of the plagioclase phenocrysts match feldspar compositions in Hole 735B gabbros. Plagioclase phenocrysts from the predominant type 2 basalts in the Indian Ocean are strongly bimodal in composition, and indicate the importance of mixing between different parental magma strains in the aggregation of the basalts (Natland, 1991; cf. Dungan and Rhodes, 1978). The group labelled 2A, having compositions more calcic than An_{78}, and its corresponding intergrown olivine–plagioclase pairs, is absent in the gabbros and corresponds to the bracket in Fig. 10A representing 'missing cumulates'. In the basalts, the 2A minerals are the largest and coarsest phenocrysts and glomerocrysts, these compositions being especially prominent in strongly porphyritic basalts. Many of the calcic plagioclases are large, irregular, sometimes rounded crystals intergrown with spinel as well as olivine. In a few basalts, such plagioclase is intergrown with magnesian clinopyroxene. Most spinel crystallized from melts more magnesian than $Mg = 60$ (based on the procedure of Allan et al., 1988 and Allan, 1993). In the rocks of Hole 735B, spinel is only found in the troctolites. The plagioclase group labelled 2B, and its co-precipitated olivine, is represented by troctolites and the more primitive olivine gabbros. Among the basalts, the 2B feldspars

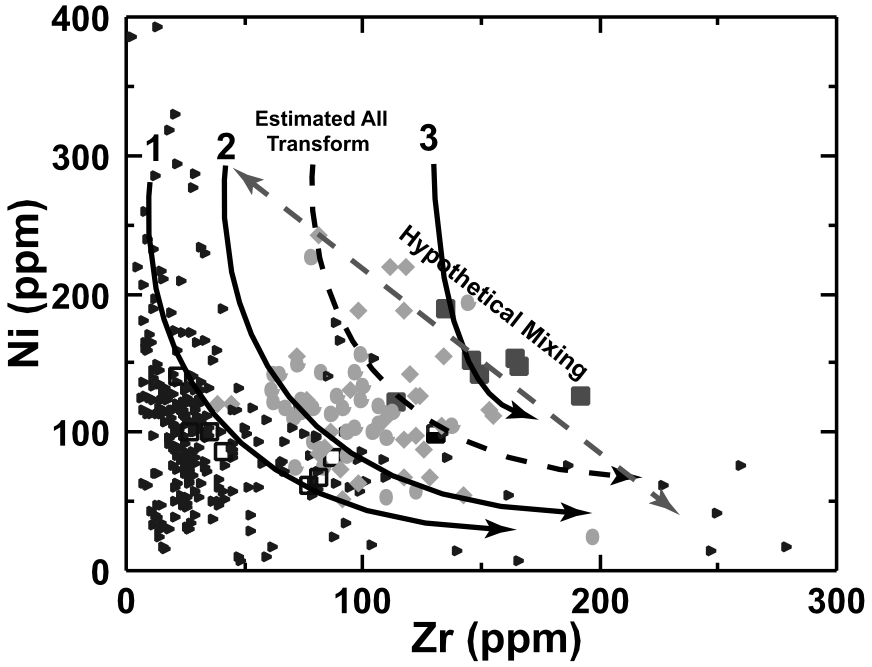

Fig. 6. Zr vs. Ni, comparing gabbros (right pointing triangles) and basalts (larger symbols, as in Fig. 10B). Curving arrows are hypothetical trends for fractional crystallization of basalt types 1, 2, and 3 of Fig. 10A, following Rhodes and Dungan (1979). The dashed line is an estimated trend for basalts of Atlantis II Fracture zone, based on limited data. Mixing between primitive and strongly differentiated liquids produces higher Zr at given Ni than the differentiation trends, as indicated by the doubled-arrowed dashed line.

comprise tabular plagioclase microphenocrysts and rims of the calcic 2A phenocrysts.

Thus olivine gabbros and troctolites of Hole 735B are representative of cumulates that crystallized during intermediate stages of differentiation of basaltic liquids found throughout the Indian Ocean, matching the typical extent of differentiation of type 2 basaltic glasses, but not the earliest stages of crystallization of primitive, parental liquids, nor the mixing history implied by the bimodal distribution of plagioclase compositions. Each of the five plutons is therefore a separate intrusive complex within which differentiation occurred after mixing and initial precipitation of refractory phenocrysts. Each pluton might have been linked to eruptions of fairly typical Indian Ocean basalts, perhaps building a sequential basalt stratigraphy of similar, moderately differentiated basalts, of the type drilled in the North Atlantic (Aumento, Melson et al., 1974; Dmitriev, Heirtzler et al., 1979; Melson, Rabinowitz et al., 1979).

Fig. 6, Zr vs. Ni, indicates the disparity between gabbro and basalt compositions in a different way. A few gabbros with very high Ni (up to 800 ppm) and Zr (up to 2000 ppm) are left out in order to show trends properly. Typical basalt differentiation trends, based on Rhodes et al. (1979), and corresponding to the three trends of Fig. 5A, are indicated, with a dashed trend shown specifically for Atlantis II Fracture Zone. This is a likely, but still mainly hypothetical, trend, since there are only four basalts from Atlantis II Fracture Zone with the requisite trace-element determinations.

Because olivine is on the liquidus of high-temperature basalts, Ni drops sharply along each curving arrow from 300 to 100 ppm, with the first small percentage of its separation. Zr increases only slightly. However, as plagioclase and then clinopyroxene join the crystallizing mineral assemblage, the curves flatten to low, but nearly constant, values of Ni, and they have strongly increasing Zr. The diagram effectively discriminates separate basaltic differentiation trends, each starting from a different parent in terms of Zr. Parental liquids that represent

very small extents of partial melting have the highest initial Zr.

Almost all gabbros of Hole 735B have too little Zr to represent basaltic liquids at any stage of differentiation from Atlantis II Fracture Zone. The main cluster of olivine gabbros (<150 ppm Ni) falls well to the left of all trends. Only oxide gabbros infested with felsic veins curve to the right. With only 15–40 ppm of Zr in most olivine gabbros, these have much less than half of the Zr expected even for the most primitive basaltic liquids found or likely along this portion of the Southwest Indian Ridge, indeed barely more than should be contained in the clinopoyroxene in the rocks. On the other hand, many gabbros have exactly the Ni and Zr concentrations necessary to drive successive liquid compositions to the right, after appropriate separation of olivine, toward high Zr, by means of cotectic crystallization of cumulus plagioclase and pyroxenes. At this stage of differentiation, the corresponding basaltic liquids were moderately differentiated.

9.2. Differentiation by deformation

In a paper now largely forgotten, Bowen (1920) once postulated that crystallization differentiation could be driven not only by gravitational movement of crystals, but also by deformation of partially molten masses of igneous rock. There is no absolute requirement that differentiation should be driven by gravitative separation of crystals from melts; physical processes, namely stresses acting on the rocks, can accomplish the same thing, especially during the later stages of differentiation. Although differentiation by deformation has not proved to be important in the study of continental layered igneous intrusions, based on Hole 735B, it appears to be a fundamental process in the ocean crust.

Bowen predicted that crystallization during deformation would result in unusually efficient separation of melt from crystals, leading to monomineralic rocks, or as more generally termed today, *adcumulates*, *of extreme purity*. Such pure adcumulates might also form *intrusives with sharp contacts* but still would not represent liquid compositions. Rock masses that experienced such deformation might have *cross-cutting lithologies which crystallized at different temperatures*, including gabbros cut by complementary *granophyric dikes and veins*. This Bowen termed *discontinuous crystallization*. The deformed rocks could develop *primary banding*, *or foliation*, while still containing abundant melt. In this way they would resemble metamorphic rocks, although having been deformed under super- rather than subsolidus conditions. Finally, very late-stage differentiates might segregate into cavities formed by *stretching or rupturing of a crystalline mesh*, there to crystallize to coarse grain size.

Bowen never imagined an application of his hypothesis to the ocean crust, but the general features of the rocks, as we have described them, clearly exemplify each of the general attributes he outlined, which are italicized in the preceding paragraph. The only one of these that needs additional comment is the first, that the gabbros of Hole 735B are adcumulates. Wager (1963) provided a geochemical criterion for adcumulates that was used by Natland et al. (1991) to characterize the upper 500 m of the Hole. It is that the rocks contain so little of any chemical constituent that is strongly excluded from the structures of cumulus minerals that only a very small percentage of trapped intercumulus material remains. Wager cited the example of phosphorus, which is known to have extremely low partition coefficients for both silicates and oxide minerals throughout almost the entire course of differentiation of a typical basaltic magma (Anderson and Greenland, 1970). Morse (1979) defined the amount of intercumulus melt retained in a rock at the point of its final freezing to be the *residual porosity*, and he showed how this can be derived using modal proportions of excluded phases such as apatite. Later, Irvine (1982) defined an adcumulate as a cumulute having <7% of post-cumulus minerals in the mode, equating this with residual porosity. Meurer and Boudreau (1998a) estimated residual porosity, which they termed *crystallized melt fraction*, or CMG, in a portion of the Stillwater intrusion using a combination of modal and geochemical data. Natland et al. (1991) mistrusted equating modal proportions determined on thin sections of coarse grained rocks from Hole 735B with chemical analyses measured on the adjacent rock chips, and in any case they lacked precise modes on most analyzed samples. They adopted Irvine's (1982) numerical criterion for adcumulates, but applied it to an entirely geochemical calculation, terming the result the *residual melt*

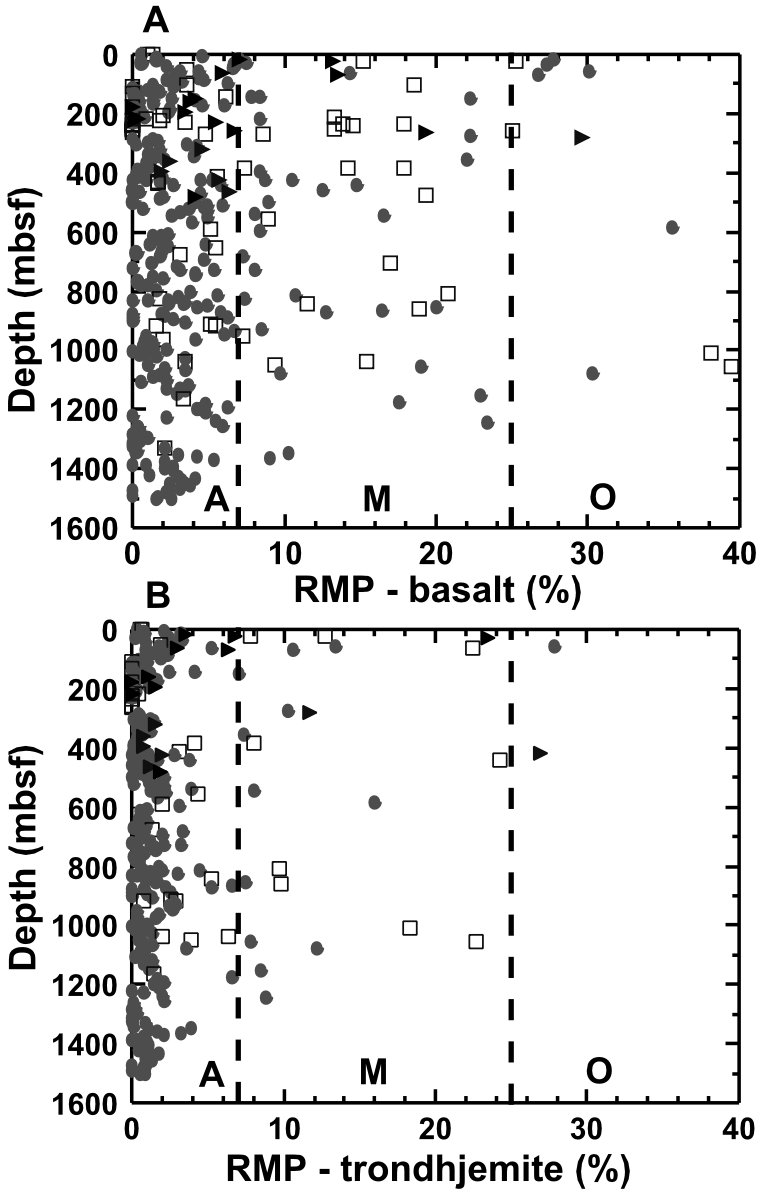

Fig. 7. Residual melt porosity (RMP) vs. depth for gabbros of Hole 735B calculated two different ways. (A) RMP is calculated by the technique of Natland et al. (1991), assuming that cumulus silicates are in equilibrium with a basaltic liquid, using trace-element partition coefficients in Bédard (1994). (B) RMP is calculated assuming that Zr not partitioned into cumulus minerals (excess Zr) is provided by a representative siliceous liquid with 700 ppm Zr. Thus Excess Zr/7 = % RMP. Oxide-bearing and oxide-rich gabbros (with >1% TiO_2) are open squares. Olivine gabbros and troctolites (<1% TiO_2) are gray dots. Dashed lines give boundaries between (A) adcumulates, (M) mesocumulates and (O) orthocumulates (Irvine, 1982).

porosity (RMP), to distinguish it from the estimate by mode. Taking Zr as the most precisely measured and least mobile during alteration of the strongly incompatible elements measured by XRF techniques during Leg 118, Natland et al. (1991) calculated an average RMP for 30 olivine gabbros analyzed during Leg 118 of 1.4%. Similarly low values were calculated for most oxide gabbros using P_2O_5

contents, which in many samples was below detection limits.

Fig. 7A shows RMP calculated for the entire 1508 m of Hole 735B, following the procedures of Natland et al. (1991). During Leg 176, there were difficulties making a complete background correction for Zr, resulting in reported values (in Dick et al., 1999b,c) that are systematically 10 ppm too high. Fig. 7A allows for this. Most rocks have less than 7% RMP, thus are adcumulates (Irvine, 1982). About half of the rocks have $<2\%$ RMP, therefore qualify as being adcumulates *of extreme purity*. Gabbros with $<2\%$ RMP are fairly evenly distributed, but even gabbros that can be classed as mesocumulates ($7 \leq \text{RMP} \leq 25\%$) are extremely rare in the lower third of the hole. Morse (1986) summarized the rarity of adcumulates in all but the largest of layered intrusions. Given the fairly small dimensions of each of the five principal plutonic masses in Hole 735B, and that individual masses of cooling magma never were more than a few meters thick, then some mechanism particular to the ocean crust at this ridge, and not exemplified by any large layered intrusion, caused extraordinarily low residual melt porosities throughout almost the full range of gabbro compositions. Natland et al. (1991) argued that this must be deformation.

The procedure for calculating RMP assumes that there is a certain amount of the Zr measured in the sample that, not fitting into a calculated mass of crystals in the rock, must reside in minerals crystallized from trapped melt of whatever *basaltic* composition was in equilibrium with the principal silicate mineral phases. This is termed the *excess* Zr, and the ratio of this excess Zr to that of the basaltic liquid estimated to be in equilibrium with the cumulus assemblage, based on known concentrations in MORB, is the fractional melt porosity. The bulk composition is therefore taken to be a binary mixture of cumulus minerals and those liquids, although the trace-element data can be used to evaluate departures from this simple assumption (cf. Meurer and Boudreau, 1998a), as follows. If the noncumulus component were more differentiated than the equilibrium basalt composition, as perhaps having been added to the rock by late veining of some very highly differentiated material such as trondhjemite, then the calculation based on a mafic liquid would only provide an *upper* estimate to RMP. As it turns out, almost all olivine gabbros that are not adcumulates based on the calculation for excess Zr have more — some of them greatly more — Zr and Y than they should. This is evident because the proportions of both elements to Ti do not change significantly through the full range of differentiation known for Indian Ocean basalts (Fig. 8A). They only begin to change after oxides join crystallizing mineral assemblages, which reduce the proportion of Ti in residual liquids, whereas both Zr and Y continue to increase (eastern Pacific liquid trend in Fig. 8A).

Fig. 8B shows that the proportions of Y, Zr and Ti in many olivine gabbros and some oxide gabbros of Hole 735B are not those of basalts, but instead those of strongly differentiated silicic liquids. Note that mixing between basaltic liquids and clinopyroxene in cumulates precipitated from those liquids does not significantly change the proportions of these three elements no matter what the mixing proportions, thus all such mixes would plot atop the basalt field in Fig. 8B. Only involvement of some non-basaltic liquid, or clinopyroxenes precipitated from such a liquid, can change this. However, only four gabbros have proportions of these elements matching those of clinopyroxenes crystallized from andesitic to rhyodacitic liquids (open arrows in Fig. 8B). All other olivine gabbros and troctolites analyzed from Hole 735B are thus adcumulates without qualification, or they are adcumulates in which the composition of the *melt finally trapped* was not basaltic, but granitic (*s.l.*). RMP based on this assumption (Fig. 7B; see caption for calculation procedure) is systematically lower than in Fig. 7A. In several samples, however, the concentration of Zr and Y even exceeds that of likely residual silicic liquids in the MORB system (e.g. DeLong and Chatelain, 1990), indicating that collection or accumulation of late mineral phases with extreme concentrations of these elements, such as zircon, occurred. These plot below the trend for silicic liquids, toward the Zr corner of the ternary in Fig. 8B.

Most oxide gabbros trend toward the Ti corner, apparently expressing simple addition of ilmenite to cumulus assemblages containing clinopyroxene precipitated from basaltic liquids. This surprising relationship suggests that there was infiltration of oxide-precipitating liquids through previously formed, more primitive gabbroic cumulates. However, this is in accord with the seam-like aspect of most oxide

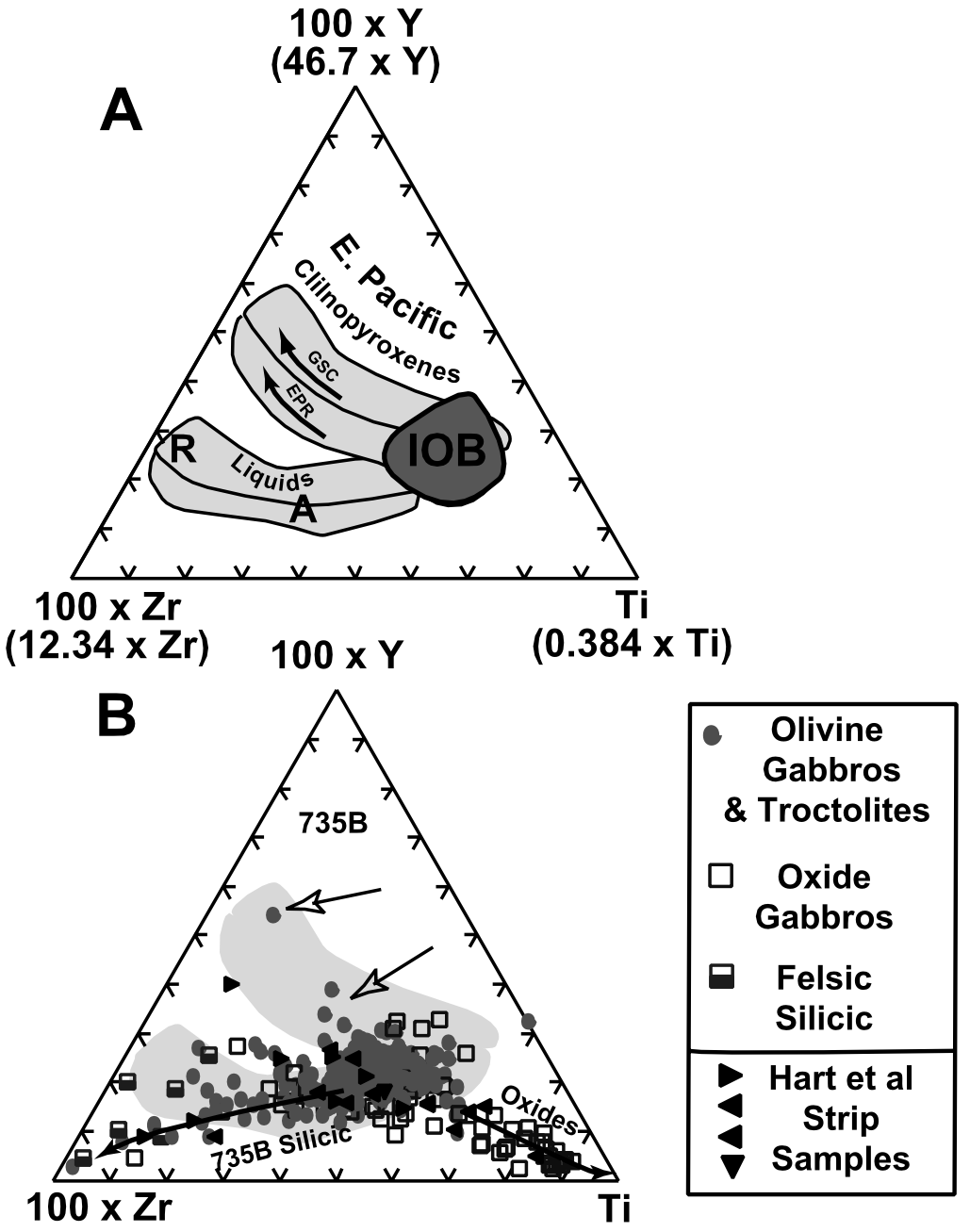

Fig. 8. Ti–Y–Zr Ternary diagrams showing effects of extended differentiation on the proportions of these elements in (A) basaltic liquids and differentiates; and (B) gabbros of Hole 735B. Proportions of Y and Zr are multiplied X 100, to expand the plotted ranges of data fields. Fields in A are based on data from the literature for MORB from the Indian Ocean (IOB) and MORB plus differentiates from the Galapagos Spreading Center (GSC) and the East Pacific Rise (EPR). The letters A and R indicate approximate locations of andesite and rhyodacite in the liquid field. The field for clinopyroxenes in A is calculated using partition coefficients from Bédard (1994), given in the bracketed variate labels. The field for Indian Ocean basalts (IOB) plots atop calculated proportions for high-Ti clinopyroxenes calculated for basaltic liquids. In B, many gabbro samples also overlap the high-Ti end of the upper shaded field for clinopyroxenes, but with a minority of samples projecting toward the Zr and Ti corners of the ternary (solid arrows). A few gabbros have proportions of these elements matching those of clinopyroxenes that crystallized from siliceous, low-Ti, liquids (open arrows).

gabbros, with the wide modal variance of ilmenite and intergrown magnetite, and with petrographic observations, to be discussed. Based chiefly on low P_2O_5 contents, however, most of even these rocks are adcumulates, with the precipitated oxide minerals adding to cumulus assemblages. Six oxide gabbros have 1–3% P_2O_5 contents; these have somewhat high Y (50–140 ppm), with concentrations correlating with P_2O_5 contents, because they contain cumulus apatite.

In summary, almost all gabbros of Hole 735B are adcumulates *of excessive purity*. About 15% of those analyzed are leavened by a little bit of silicic differentiated liquid, which is otherwise evidenced by over 200 silicic/felsic veins distributed throughout the core. Presumably the silicic material in the gabbros penetrated and perhaps slightly expanded intergranular porosity structure of nearly ideally pure cumulates.

Dick et al. (1991b) used the term *synkinematic differentiation* to describe the confluence of deformation and igneous differentiation that occurred in the upper 500 m of Hole 735B. Neither they nor any other members of the Leg 118 scientific party were aware of Bowen's (1920) description of the effects of combining crystallization differentiation with deformation, nor of his term for this. Bowen's concept itself can be traced from Barrow (1892, 1893), through Harker (1904, 1909), then Bowen, and then to Daly (1933), among early workers. Both Harker and Daly had different names for it. What is important now is not whether filter pressing (Harker), differentiation by deformation (Bowen), wine-press differentiation (Daly), or synkinematic differentiation (Dick) is the term of choice, but the understanding that, by virtue of the wide areal distribution of the products of slowly spreading ridges, all these terms stand for a major process acting in the formation of ocean crust and of the overall differentiation of the Earth.

9.3. Patterns of differentiation and melt migration

The numerous cross-cutting oxide gabbros, that are the main examples of Bowen's discontinuous crystallization, represent the product of extended high-iron differentiation of parental basaltic liquids (e.g. Natland et al., 1991; Ozawa et al., 1991), and the thick sequence of them near the top of the hole must reflect complex processes of coalescence from a large volume of crystallizing rock. The troctolites and olivine gabbros comprising the bulk of the five plutons sampled at Hole 735B are deficient in the very geochemical constitutents that are so concentrated in the oxide gabbro seams and felsic veins. This suggests that iron-rich liquids were expelled from the crystalline matrix of the several plutons beneath or adjacent to the hole by the interactive processes of differentiation by deformation. That the olivine gabbros and troctolites are adcumulates indicates that the process was extremely efficient.

Construction of the lower crust thus began with injection of a series of stacked plutons, each now consisting of dozens to hundreds of much smaller intervals of troctolite, olivine gabbro and gabbronorite adcumulates. Each pluton was intruded into its own physical space, but the order of the initial stage of each intrusion has not yet determined. The entire mass could well have been partly molten during the entire sequence of intrusion, thus each interval had the potential to contain some residual melt, which could reach an extremely differentiated, iron-rich or even granitic composition whenever the temperature dropped low enough. Temperatures clearly did drop this low, therefore granitic veinlets formed even near the base of the section. Such melts would have tended to concentrate ahead of solidification fronts within each small crystallization interval (Marsh, 1995), but also to flow into fractures or intergranular porosity structure as these developed during the course of deformation. Thus compaction and perhaps deformation eventually led to quite complete expulsion of the strongly differentiated melts from most of the material, and to their concentration along numerous small gashes, fractures, or other porosity structure. For this reason, most oxide gabbros occur as crosscutting, intrusive seams.

Although each pluton was separately intruded as numerous small injections of magma, each one nevertheless has more differentiated, less magnesian, gabbro toward the top (Fig. 3A). This arrangement is not likely to have resulted from preferential injection of more differentiated magma from some depth below. Instead it indicates that there was probably reaction within each pluton between a largely crystalline and compacting cumulus matrix before it became rigid, and the buoyant, upward- migrating melt being expelled from that matrix and differentiating through time as each pluton cooled. Indeed, the rock-to-rock

variability just within, say, 20 m intervals of troctolites and olivine gabbros, given by the spread in Mg shown in Fig. 3A, is fairly broad, indicating that the reaction process was likely concentrated in channels or narrow zones of filtered flow, just within the compacting plutons. Only after sufficient melt, at least 50% (Marsh, 1995), was expelled from each pluton could they have become rigid enough to fracture and become intruded by the even more differentiated melts that produced the seams of oxide gabbros. The typical sharp contacts, however, suggest that the olivine gabbros and troctolites were adcumulates, or nearly so, before this fracturing occurred.

The unusual concentration of oxide gabbros between 200 and 270 mbsf indicates that this one portion of the cored section was a favored zone of coalescence of migrating highly differentiated melts. However, this interval was never completely, nor perhaps even largely, molten inasmuch as it contains several screens of olivine gabbro, and the seam-like aspect of the oxide-rich gabbros, and their sharp contacts, are still evident. This zone is primarily a composite of multiple small oxide concentrates or seams. No one of these ever contained more than a few meters thickness of mobile magma; most seams probably held much less than that.

Since oxide gabbros represent the residua of perhaps 80–90% crystallization differentiation from a primitive, parental basaltic liquid (e.g. Clague et al., 1981; Juster et al., 1989), the rocks of this 70 m-thick interval clearly had to coalesce from a much larger volume of cumulates (i.e. an equivalent vertical column 350–700 m thick). The olivine gabbros in the lowest 300 m of the hole which are so nearly devoid of oxide-rich seams (Figs. 2 and 3B) may be part of that volume of cumulates, although lateral migration of differentiated melt could also have produced the thickened zone of oxide gabbro. The pattern of melt migration was influenced by differences in density between melt and surrounding rock, as discussed below.

9.4. The role of melt density

In Fig. 9A, the Mg#'s of experimentally produced MORB glasses (Walker et al., 1979; Dixon and Rutherford, 1979; Juster et al., 1989) are plotted vs. their densities, as calculated using the procedure of Niu and Batiza (1991). A regression is calculated for compositions within the gray band (see caption). Fig. 9B shows compositions of coexisting olivines and both pyroxenes in Hole 735B gabbros, from Leg 118 data sources, and regressions for each. These allow use not just of olivine, but also, in gabbros without olivine, of orthopyroxene or clinopyroxene as a means of estimating liquid Mg#, by substitution into the olivine–liquid relationship of Roeder and Emslie (1970). Then, using the relationship in Fig. 8A, an *analog* density for the relevant basalt glass for each gabbro for which these mineral compositions have been determined, thus far only from the upper 500 m of the hole, can be plotted vs. depth, as in Fig. 8C. Analog melt densities for compositions of all but oxide gabbros can also be estimated, assuming that the bulk Mg# of the gabbro (from XRF data) is that of clinopyroxene, the most abundant ferromagnesian silicate in the rocks. These do not differ appreciably at any depth from analog densities calculated from mineral data (Fig. 9C). For oxide gabbros, because oxide minerals tend to reduce Mg# of the host rock, the Mg# of clinopyroxene is taken to be normative DiEn/(DiEn + DiFs), and this is used to estimate the density of the analog equilibrium melt. On this basis, estimated analog densities of liquids that produced all gabbros range from 2.66 to 2.77 g cm^{-1}. Some densities could have been higher if the gabbros precipitated from iron-rich immiscible liquids comparable to those in Fig. 9A. The analog density of trondhjemite is taken as 2.5 g cm^{-1}, from Fig. 9A.

What is the relationship of the densities of analog liquids to their surrounding crystalline matrix at the time of final crystallization? To first order, we need an estimate of densities of gabbros at the temperature of the last liquids in equilibrium with them, at their lowest residual melt porosity. Temperatures of those liquids can be estimated in the same way as liquid densities, using a regression as a function of Mg# based on experimental liquids, and again excluding immiscible experimental liquids, whether very iron-rich or siliceous (Fig. 9D). Fig. 9E plots normative densities of hot rocks, based on CIPW norms, and at the temperatures of the analog liquids in equilibrium with cumulates, against depth. Densities of normative minerals are corrected for temperature, using the thermal expansion coefficients of Lange and Carmichael

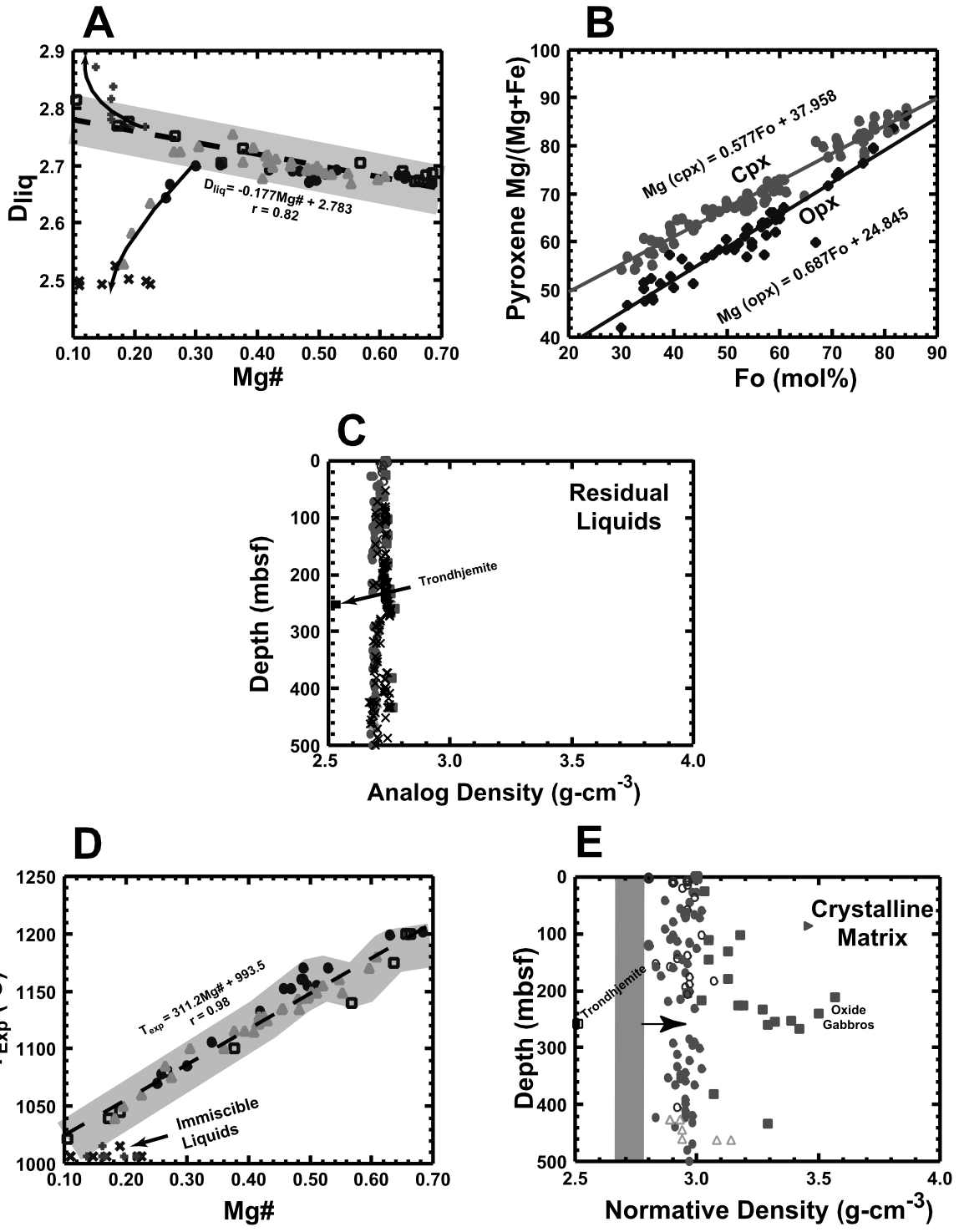
A
Dliq
Mg#
D_{liq}= -0.177Mg# + 2.783
r = 0.82
B
Pyroxene Mg/(Mg+Fe)
Fo (mol%)
Mg (cpx) = 0.577Fo + 37.958
Cpx
Opx
Mg (opx) = 0.687Fo + 24.845
C
Depth (mbsf)
Analog Density (g-cm^{-3})
Residual Liquids
Trondhjemite
D
T_{Exp} (°C)
Mg#
T_{exp} = 311.2Mg# + 993.5
r = 0.98
Immiscible Liquids
E
Depth (mbsf)
Normative Density (g-cm^{-3})
Crystalline Matrix
Trondhjemite
Oxide Gabbros

(1990). Even at magmatic temperatures, however, there is very little difference between the normative densities and the bulk densities of most samples measured at room temperature and atmospheric pressure onboard *JOIDES Resolution*.

Comparison of Fig. 9C and E shows that densities of even the most iron-enriched parental analog liquids produced during experimental studies are much less than both the normative (and measured) densities of all varieties of gabbro from Hole 735B. Thus expelled intercumulus melts, even those within oxide gabbros, were strongly buoyant within their crystalline matrix, and would have migrated upward as porosity structure developed during deformation. If perhaps differentiation attained a stage of immiscible separation of siliceous and very iron-rich liquids, then *some* of them might have attained densities of 2.9 g cm^{-3} (Fig. 9A), matching densities of olivine gabbros. The one place in the section where this might have occurred, based on mineral compositions in two samples, is indicated by the arrow in Fig. 9E. All other oxide gabbros, crystallized from less dense liquids that were buoyant in their surroundings. This analysis does not take into account the role of volatiles in reducing melt density, which would have made even iron-rich melts still more buoyant. Consequently, Fig. 8E points overwhelmingly to melt buoyancy as a factor in the differentiation of these rocks, with only the merest possibility that neutral buoyancy was achieved by some highly differentiated melts within the gabbroic portion of this block of ocean crust.

A consequence is that the strong concentration of oxide gabbros between 200 and 270 mbsf represents a *physical* arresting of the tendency for upward flow of differentiated magma in these rocks. That is, there must have been a permeability barrier at about 200 mbsf. We speculate that the rocks above this may have been colder, although not necessarily completely frozen, because of the downward influence of hydrothermal cooling, thus that they formed a nearly completely solidified caprock, through which migrating melts could not penetrate. Alternatively, melt migration may have been deflected beneath a zone of shear that produced impermeable barriers by means of the reduction in grain size that is so evident in the many porphyroclastic to mylonitic gabbronorites and oxide gabbros from 0 to 200 mbsf. At the same time, shear may have accentuated formation porosity, thus provided avenues for flow, perhaps along the several breccias which occur within some of the most oxide-rich gabbros (Robinson et al., 1989).

Compare this now to Hess Deep, representing the fast-spreading East Pacific Rise. There, highly differentiated magmas produced gabbronorites and oxide gabbros just beneath the base of the dikes, in an interval interpreted to be the frozen remnants of a

Fig. 9. Comparison of the densities of estimated melts last in equilibrium with gabbros, and their crystalline matrix at melt temperatures, at the point of final expulsion of residual melt. (A) Mg#($= Mg/[Mg + Fe^{2+}]$, where $Fe^{2+}/[Fe^{2+} + Fe^{3+}] = 0.86$) vs. densities of experimental MORB liquids (filled circles — Walker et al., 1979; open squares, +'s, and x's — Dixon and Rutherford, 1979; gray triangles — Juster et al., 1989), as calculated using the procedure of Niu and Batiza (1991). Analog densities for liquids which produced the gabbros of Hole 735B are calculated from the regression shown, which is based on data points included in the shaded area, and which excludes immiscible segregates (x's and = 's) and other siliceous compositions along the lower curved arrow. (B) Correlation between Mg/(Mg + Fe) of pyroxenes and Fo content of intergrown olivine in Hole 735B gabbros (Ozawa et al., 1991; Hébert et al., 1991; Stakes et al., 1991; Natland et al., 1991). These correlations are used to calculate Mg# basaltic melts in equilibrium with these minerals in gabbros lacking olivine, or from olivine itself where it has been analyzed, using regressions shown in the figure, from the relationship between olivines and basaltic liquid of Roeder and Emslie (1970), assuming $K_D = 0.28$ (Hébert et al., 1991). From the Mg#'s, analog densities can be calculated. (C) Analog densities of liquids in equilibrium with Hole 735B gabbros vs. depth. All solid symbols are based on calculations using olivine, orthopyroxene and clinopyroxene. Most X's are calculated from whole-rock (XRF) compositions, assuming that Mg# of the rock = clinopyroxene in the gabbro.. Oxide gabbros are excepted because abundant ilmenite and magnetite influences Mg#. For these instead, the calculation is based on normative $Di_{En}/(Di_{En} + Di_{Fs})$. (D) Temperature of experimental MORB liquids of A, vs. Mg#. The regression is calculated from all data points in the shaded area (excluding immiscible liquids), for use in E. (E) Normative densities of gabbros calculated at their temperature of crystallization, based on Mg#'s for liquids calculated from mineral Mg#'s and regressions in B, or olivines directly, using the relationship of Roeder and Emslie (1970). Normative mineral densities are adjusted for temperature using the thermal expansion coefficients of Lange and Carmichael (1990). Open triangles are troctolites, dots are olivine gabbros, open circles are gabbros with $0.5\% < TiO2 < 1\%$; filled squares are oxide gabbros with $\geq 1\%$ TiO_2. The shaded region gives the range of analog liquid densities, from C. The arrow indicates where the maximum density of immiscible iron-rich liquids, about 2.9 g cm^{-3}, from A, might have matched densities of olivine gabbros in the section.

melt lens (Natland and Dick, 1996). These rocks are comparable in silicate mineral compositions to the oxide gabbro seams of Hole 735B. However, none is nearly so oxide rich. Because the melt lens is a steady-state feature at the East Pacific Rise, melt migration clearly has a persistent and uninterrupted path to the top of gabbro cumulates. In part this is because there are no significant faults penetrating into the gabbros, consequently the effective depth of the basalt solidus never reaches into rock below the melt lens, while it exists, and underlying gabbros are not deformed. At Hole 735B, on the other hand, infrequent magma supply more than once may have allowed the basalt solidus to descend well into the crystallizing mass of gabbros.

At Hess Deep, in the absence of faulting and deformation-related impedances to upward melt migration, the vertical porosity profile depended only on compaction of cumulates and lateral crustal dilation in the narrow column of rock immediately beneath the lens. The process of melt reaction during early melt expulsion from the base of the stack of cumulates, described above as occurring within each individual pluton at Hole 735B, acted instead throughout the entire column of gabbro at Hess Deep. Thus whereas the gabbros of Hole 735B may be considered a large stack of sub-horizontal, irregularly-injected, widely-distributed solidification fronts (Marsh, 1995) that were disrupted by shear deformation during crystallization, the section at Hess Deep effectively represents a single *vertical* solidification front, narrowing toward the melt lens, that acted throughout 4 km of rock, and which was never laterally disrupted. Because the gabbro column at Hess Deep was, in a steady-state fashion, persistently hottest at its base and coolest at the top, all buoyant residual melt tended to flow upward, concentrate, and be most differentiated, at the melt lens (Natland and Dick, 1996). At Hole 735B, the coalesced and highly differentiated melts that formed the oxide gabbros between 200 and 270 mbsf were the nearest thing to a melt lens that this very slowly spreading, colder, sporadically magmatic, and actively deforming ridge could produce. There never was much melt beneath the rift valley at any one time, and to the extent that it coalesced, it did so within, not at the top, of the gabbro column. A counterpart today might be very difficult to detect seismically. Impedance contrasts in the cold rock, however, suggest that the interval of oxide gabbros might produce a seismic reflector within Layer 3 (Itturino et al., 1991).

9.5. Relationship between deformation and the distribution of oxide gabbros

We can now be more precise about the relationship between deformation and the distribution of oxide gabbros in the rocks of Hole 735B, particularly in the thick zone of oxide gabbros between 200 and 270 mbsf. Throughout most of the gabbros below this, the most characteristic manner of concentration of oxide minerals is in individual seams no more than 1–5 cm thick, or in clusters of such seams. A typical example is shown in Fig. 10A, from a depth of 809.4 mbsf. The oxide minerals are arranged along a fracture that is distributed over a zone about 1 cm wide. It is not a sharp fracture, which broke pre-existing silicate mineral grains. Rather, the oxides are arranged along the irregular boundaries of plagioclase and clinopoyroxene, which formed the principal lines of weakness while the fracture formed, and are dispersed somewhat between them. The fracture represents porosity structure that opened in a nearly solid, but weak, aggregate of crystals, and along which a melt that was precipitating oxide minerals could percolate.

Fig. 10B depicts an oxide gabbro from much higher in the hole (100.9 mbsf), and shows the tendency of abrupt changes in grain size in controlling the distribution of percolating melts that precipitated oxide minerals. To show the full distribution of oxide minerals in the thin section, the migrograph on the left uses heightened-contrast to show the distribution of oxides (black) in their matrix of silicates (white). The inset on the right is a standard transmitted-light photomicrograph that shows the grain-size contrast among the silicate minerals above and below the upper seam of oxide minerals. The rock itself is barely deformed, except to say that it was subjected to forces that opened porosity structure along pre-existing lines of weakness in the partly molten rock. Fig. 10C, from 252.5 mbsf in the main zone of oxide gabbros, is an oxide gabbro in which the oxide minerals are concentrated along arrays of fractures. Again, oxides only are selected. Arrows indicate alignments of oxide minerals along fractures. There are three fracture

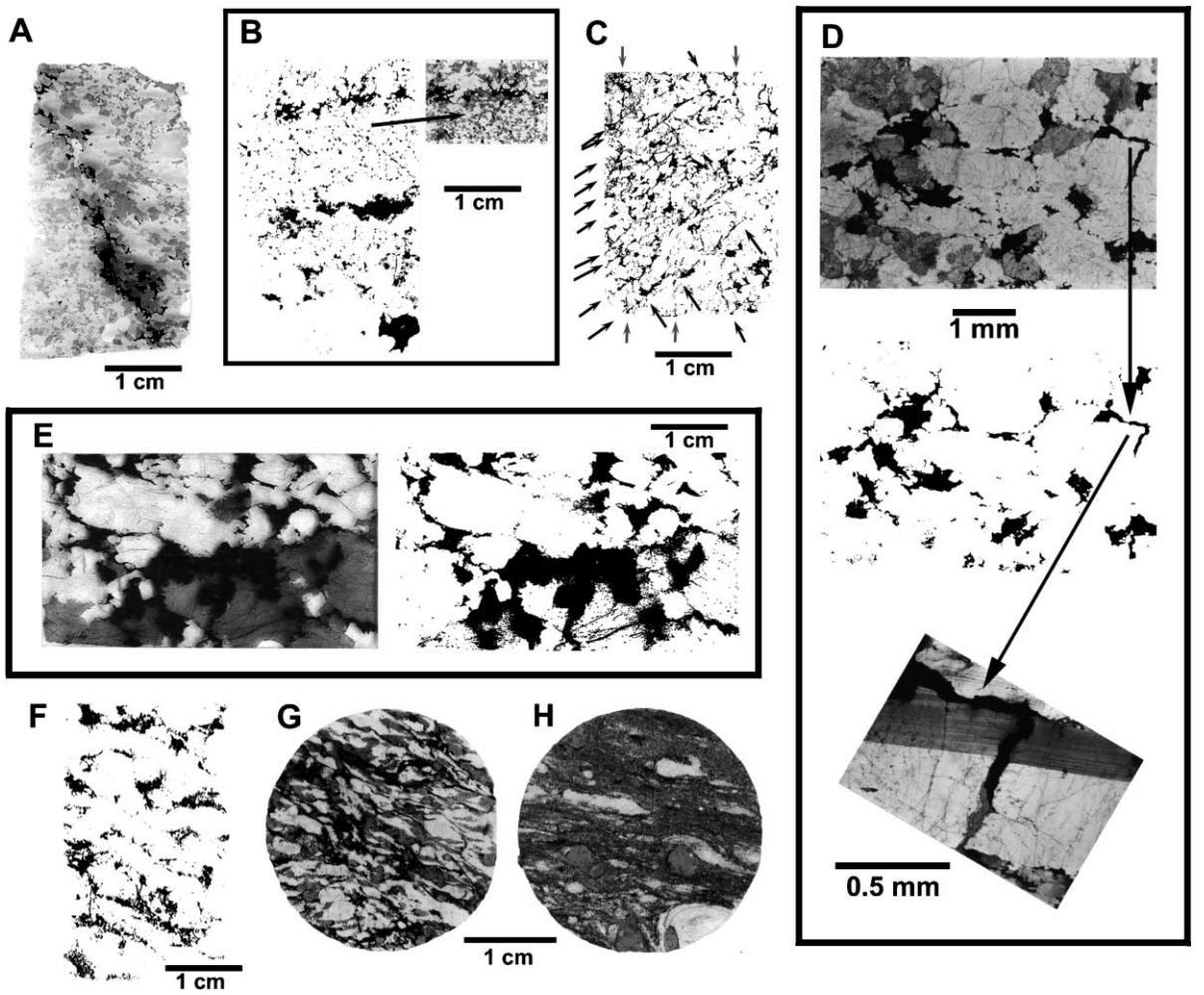

Fig. 10. Examples of the relationship between structure and the placement of oxide gabbros in Hole 735B. (A) Sample 176-735B-130$-4, 123–127 cm. Full thin section scanned in transmitted light. (B) Sample 118-735B-23R-1, 46–53 cm. Full thin section scanned in transmitted light, with contrast enhanced to delineate the distribution of oxide minerals (black) against their silicate matrix (white); inset, photomicrograph of a portion of the slide in plane polarized light, showing grain-size contrast above and below the upper seam of oxides, with clinopyroxene = gray and plagioclase = white. (C) Sample 118-735B-52R-4, 88–94 cm; full thin section scan of oxide gabbro, with contrast enhancements to show distribution of oxides (black) against the silicate matrix (white); arrows are as described in the text. (D) Sample 118-735B-51R-1, 102–104 cm. Top panel is a photomicrograph in plane polarized light; middle panel selects oxides; lower panel is a close-up of a portion of the slide, indicated by the arrows, in cross-polarized light. (E) Sample 118-56R-2, 103–120 cm, oxide gabbro. Left panel is a full thin section scan in transmitted light. Right panel selects oxides. (F) Sample 118-735B-82R-5. Full thin section scan of an oxide gabbro with gneissic texture; oxides selected. (G) Sample 118-735B-53R-3, 15–17 cm. Scan in transmitted light of a thin section taken from a minicore of neissic oxide gabbro. No contrast enhancement. (H) Sample 118-735B-56R-2, 11–14 cm. Scan in transmitted light of a thin section from a minicore of a gabbro cataclasite. No contrast enhancement.

arrays, the most prominent of which is oblique to the plane of the thin section, as indicated by the arrows on the left side of the micrograph. There is a weaker array of fractures orthogonal to this, and another that is even weaker arranged vertically. The section shows the general tendency for porosity structure to have opened along sets of fractures, breaking up the silicate matrix into fracture-bounded pieces, around which the oxide minerals then precipitated from percolating melts. In many cases, the fracture-bounded pieces of silicates

were previously deformed, being extensively recrystallized and even foliated. Those patterns, however, are now obscured by the pattern of cementing oxide minerals.

Additional examples of the tendency of oxide minerals to precipitate around rectilinear fragments of silicates are shown in Fig. 10D and E. In Fig. 10D, the pattern of disruption of silicates is still strongly controlled by pre-existing grain boundaries between pyroxenes and plagioclase, but in one case, blown up in the lower panel of the figure, a coarse plagioclase grain was fractured through its center before oxide minerals precipitated in the resulting cavity. Fig. 10E is a rock in which fractures created a great deal of porosity, resulting in cavities that allowed >20% of oxide minerals to concentrate in the area of the thin section. The blocky aspect of the silicate fragments is still apparent, but in some cases these are now virtually matrix-supported by the oxide minerals. In rocks with gneissic fabric, fractures followed the foliation planes, and were the principal loci of precipitation of oxide minerals (Fig. 10F and G).

Rocks with extreme crystal–plastic deformation occur at several intervals within the thick zone of oxide gabbros (Fig. 10H), but do not necessarily have abundant oxide minerals. The rock shown in Fig. 10H is only 0.9 m above the massive oxide gabbro of Fig. 10E. The gneissic rock of Fig. 10G is only 3 m below the fractured, but non-foliated, rock of Fig. 10C. On a scale of several meters in the massive oxide gabbros, there are several cycles in which the rocks grade downward from fractured, but otherwise undeformed, and quite oxide-rich, through gneissic and porphyroclastic rocks, and then finally to thin cataclasites. It is quite clear that the *quantity* of oxide minerals is greatest in the rocks which were fractured, but not intensely sheared, but also that the structure of the fractured, oxide-rich rocks is closely related to the zones of shear. The distribution of stresses was obviously complex. Melts precipitating oxide minerals concentrated in the rocks with the greatest fracture dilatancy, and probably could not pass through rock that experienced radical grain-size reduction. As buoyant melts arrived from below, zones of rock beneath permeability barriers were likely subjected to magmatic overpressure, with the only relief coming from dilatant expansion of the underlying more permeable rocks. Effective stress would have been reduced and strain localized by, as Bowen (1920) described it, *stretching or rupturing of a crystalline mesh*, with the rupturing melts crystallizing to coarse grain size (coarse ilmenite–magnetite–sulfide intergrowths).

The connection between oxide-rich gabbros and zones of deformation is thus intimate, but there is no correlation between modal proportions of oxide minerals and the intensity of crystal–plastic deformation. Since the final minerals to crystallize in these rocks, both from the perspectives of idiomorphic relationships and patterns of fracturing, were oxide minerals (plus associated globular sulfides), the textures of all the rocks shown in Fig. 10 formed while the rocks were still partly molten, and more than likely from about 1100–1000°C, when oxide minerals are on the liquidus of differentiated melts derived from parental abyssal tholeiite (DeLong and Chatelain, 1990).

9.6. The link between discontinuous crystallization and continuous differentiation

How did magmatic differentiation work at Hole 735B? Complexity arises because of the extraordinary crosscutting nature of the different lithologies. Leaving aside the felsic veinlets, all gabbroic lithologies are cumulates, at least in a geochemical sense. The several bodies of troctolite and olivine gabbro crystallized from typical Indian Ocean basaltic magmas, and while crystallizing, they probably served as staging areas for eruptions that entrained some of the crystallizing minerals as phenocrysts. Eventually, however, most residual melt was expelled/removed/squeezed from them. Where did it go? It went first into oxide-gabbro seams. These, too, qualify as ilmenite–magnetite rich *adcumulates*, being almost totally deficient, for example, in P_2O_5. Their particular interstitial liquid, which carried the phosphorus, was also almost systematically expelled/removed/squeezed from the rocks. But these liquids never erupted. Where did they go? Into even more evolved oxide gabbros, some with apatite, and trondhjemites. There are, indeed, six analyzed oxide gabbros which contain >1% P_2O_5, thus they have *cumulus* apatite. However, even these do not have

much Zr. That is sprinkled around in felsic/trondhjemitic veinlets.

In summary, of the three potential components which might make up any gabbro of Hole 735B — a cumulus matrix of crystals separated from basaltic melts, minerals which crystallized from trapped basaltic melts, and extreme differentiates, only the first and third appear to be geochemically important. That is, most rocks are gabbroic adcumulates (troctolites to oxide gabbros) intruded in hundreds of places by extreme ferrogabbroic/felsic/trondhjemitic material (Fig. 3). Even in olivine gabbros, the compositions of *melts finally trapped*, when present in sufficient quantities to measure, are those of broadly granitic liquids, producing such things as excess Zr and Y, beyond that expected for typical basaltic melts. This is Bowen's *discontinuous crystallization*, carried into almost every sample, in the course of *differentiation by deformation*. The differentiation process was continuous, but the resulting rocks are a discontinuous shuffling of varieties of gabbroic adcumulates, not one of which approaches a liquid composition.

9.7. Sedimentary analogs of cumulus processes at Hole 735B

A useful way to consider the spectrum of cumulus processes that act in the ocean crust is in comparison to sediments. Jackson (1961) likened igneous cumulates of the Stillwater ultramafic zone to varieties of chemical sediments, arguing that precipitate mineral grains grew as they settled, and that afterward they were cemented by crystallization from pore fluids. The usual assumption for a layered intrusion is that minerals precipitate on the floors, walls, and roof of some substantial magma body, whether in the form of a rain of gravitationally settled mineral grains, or in the manner of crystals of sugar nucleating on and growing from the surfaces of a beaker. Most textural interpretations of cumulates, including the origin of layering, and many hypotheses about the origin of adcumulates (e.g. summary of Morse, 1986), stem from this assumption. These explanations can, by analogy to sedimentary rocks, be termed *hardground* hypotheses, since they all seek to explain how residual melt porosity is reduced virtually to nil in a boundary layer, which may only be a few meters or even centimeters in thickness, at the interface between the magma body and the gathering cumulus minerals. According to Morse (1979, 1986), in order to develop adcumulates in these circumstances, the larger and more slowly cooled the magma body the better.

Recent studies place more stress on the role of post-cumulus compaction and textural re-equilibration in reducing melt porosity in fairly thick crystal mushes in large layered intrusions (Hunter, 1998) including Rhum (Bédard et al., 1988) and the Stillwater complex (Meurer and Boudreau, 1998a). However, fairly large and thick sheets of magma are still required to produce continuity of layering over great distances at Stillwater (McCallum, 1996), Great Dyke (Wilson, 1996), and the Bushveld Complex (Eales and Cawthorn, 1996). Skaergaard continues to be viewed as the result of injection of a single, prolonged pulse of magma (McBirney, 1996; Irvine et al., 1998). In many cases, the magma bodies were large enough to have convected on their own, or been convectively overturned by injection of plumes of magma (Campbell, 1996), with consequences for cumulate stratigraphy. Even at Rhum, unconsolidated cumulates slumped, collapsed along faults, and were laterally intruded by picrites beneath a repetitively re-injected magma body some 4 km in diameter and 100–200 m thick (Emeleus et al., 1996). Study of these several intrusions lies at the heart of cumulate theory, yet the essential role of a major magma body is still not disputed for any of them. Most cumulates in these intrusions are described as floor cumulates, and the adcumulates within these developed by upward escape or migration of intercumulus melt toward the overlying magma bodies. The consolidating cumulates at most are viewed as being only a few hundred meters thick (McCallum, 1996; Emeleus et al., 1996).

In the ocean crust, adcumulates form without being near a magma chamber even so small as the one envisioned for Rhum. At the East Pacific Rise, for example, the difficulty is to maintain sufficient porosity and permeability through a consolidating gabbroic mass some 4 km thick, in a narrow column extending from the melt lens down to the mantle, in order to sustain a steady-state melt lens at the dike–gabbro transition, and at the same time add to the bulk of the gabbroic layer as spreading occurs, with the majority of the rocks in the column becoming adcumulates. Natland and Dick (1996) consequently stressed the inadequacy of hardground hypotheses

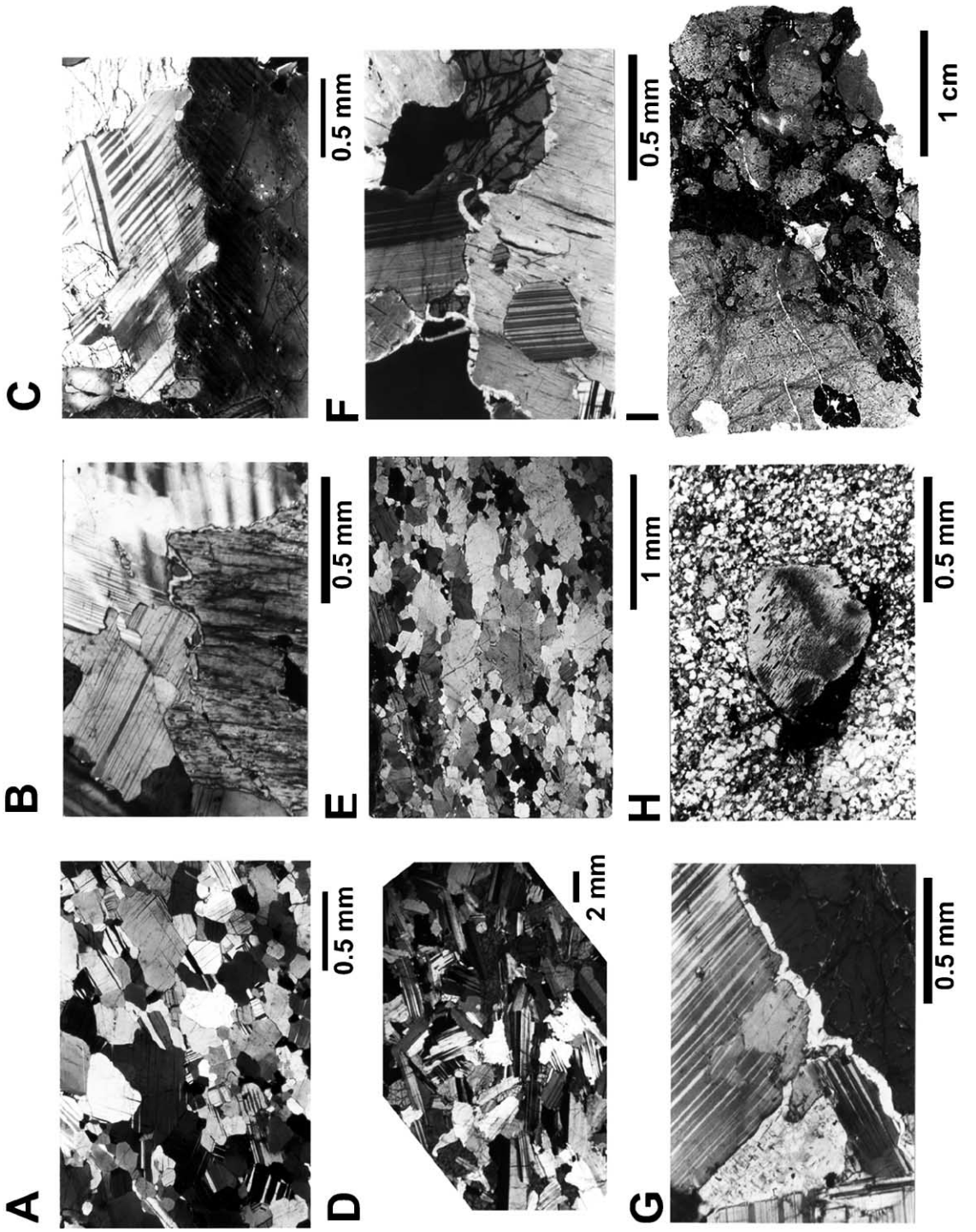
A
0.5 mm
B
0.5 mm
C
0.5 mm
D
2 mm
E
0.5 mm
F
0.5 mm
G
0.5 mm
H
1 mm
I
1 cm

for the formation of adcumulates in this environment. Instead, they argued that most of the time the upper melt lens has to rest on a nearly impermeable mat, which is to say that the underlying rocks already are adcumulates, otherwise the dense iron-rich melts within the lens would sink into underlying intergranular porosity structure. In support of this, the most recent geophysical estimates are that the crust below the melt lens at 9°48′N on the East Pacific Rise, modelled as a block 4 km thick, contains 2.5–18% melt, this uncertainty depending on melt geometry (Crawford et al., 1999). The melt lens above it contains almost pure melt. This study also revealed the presence of another melt lens near the Moho. It is estimated with some uncertainty to be about 70 m thick and 1 km wide.

Obviously, at a slow-spreading ridge, the difficulty is even greater. There is no seismically detectable melt lens at any depth (see summary by Sinton and Detrick, 1992). Yet we need to imagine an extremely efficient process of reduction in melt porosity through a thick gabbroic section, and the creation of a substantial mass of adcumulates 'of excessive purity', without even the melt lenses of the East Pacific Rise.

The appropriate sedimentary comparison is, we believe, those rocks in thick formations that attain extreme porosity reduction in the course of compaction, namely very pure quartzites and limestones. Quartzites are particularly instructive, since they are monomineralic rocks of excessive purity and may therefore be analogous to monomineralic adcumulates such as anorthosites and dunites. No one has ever proposed a 'hardground' mechanism for the formation of pure quartzites. Instead, deep burial, compaction, expulsion of intergranular fluids, and cementation are all considered important in the reduction of formation porosity to form quartzite (e.g. Pettijohn, 1975; Tada and Siever, 1989). An additional factor that is especially effective in reducing formation porosities to extremely low levels is pressure solution (Thompson, 1959; Skolnick, 1965; Houseknecht, 1987), and this process also requires a thick body of sediment. Natland and Dick (1996) invoked pressure solution to reduce residual melt porosity efficiently in the thick consolidating crystal mush at Hess Deep. Expulsion of melt and its buoyant ascent in fractures, gashes, and intergranular porosity structure toward the melt lens is the complement to formation of deep adcumulates at a fast-spreading ridge. The process is interrupted repeatedly as magma is injected from the mantle below, but eventually the consolidating rocks move away from the locus of magma injection at the center of spreading, and very low residual melt porosity is attained.

Evidence for pressure solution comes from rock textures. Comparison to the most recent hardground hypothesis for the formation of adcumulates is instructive. Hunter (1987, 1996) invoked grain boundary dissolution and reprecipitation to produce textural equilibrium, including formation of 120° grain-to-grain triple junctions. An example of textural equilibrium in a dredged gabbro from the Indian Ocean is shown in Fig. 11A. This texture is the hallmark of an adcumulate, since on an intergranular scale, it represents almost perfect expulsion of intercumulus

Fig. 11. Textural aspects of pressure solution. (A) Textural equilibrium among plagioclases in gabbro; dredged sample PROT 10D-42, Anna de Koenigh Seamount, Southwest Indian Ridge, crossed nichols. (B) 'Microstylolitic' grain interpenetration between plagioclase and clinopyroxene in olivine gabbro; ODP118-735B-72R-3, crossed-nichols. (C) Sutured grain boundary between two large plagioclases in olivine gabbro, the lower one with a strained extinction pattern; ODP118-59R-3, crossed nichols. (D) Example of texture interpreted as magmatic foliation in olivine gabbro, but with many occurrences of sutured boundaries between plagioclases; ODP176-735B-89R-2, *r*-8 cm, Piece #1, crossed nichols. (E) Olivine gabbro with fitted-fabric texture in plagioclases, combining grain flattening and sutured grain boundaries; dredged sample PROT 10D-67, crossed nichols. (F) Grain-boundary orthopyroxene, with uniform extinction, wrapping around sutured boundaries between olivine (right), clinopyroxene (lower), and plagioclase (upper center and left); ODP118-735B-75R-3, olivine gabbro, crossed nichols. (G) Sutured grain boundary between plagioclase and clinopyroxene, with a thin band of grain-boundary orthopyroxene at uniform extinction; ODP118-735B-59R-3, olivine gabbro, crossed nichols. (H) Rounded clinopyroxene porphyroclast with 'shadow' overgrowths of oxide minerals, in oxide-gabbro porphyroclastic mylonite; ODP118-735B-56R-2, 11–14 cm, plane-polarized light. (I) Full thin section scan of a coarse oxide gabbro breccia, consisting almost entirely of clinopoyroxene (gray), locally altered to amphibole (dark gray), and oxide minerals, in transmitted light, from an oxide-rich seam at ODP-118-735B-86R-1, 104–108 cm, Piece #8A. The irregular boundaries of the coarse clinopyroxenes, and of the one plagioclase in the center, are interpreted as dissolution or resorption features, but silicate fragments are now entirely matrix-supported by oxide minerals in the breccia zone.

melt. This mechanism, however, does not result in any shift of position of the centers of the original large cumulus minerals. They are still where they came to reside against each other following some amount of simple uniaxial compaction, but with almost all the original intergranular porosity now filled in by reprecipitated mineral material. Indeed, one would not expect the centers of crystals in an original network of cumulus minerals to shift if they were cemented at a hardground with no significant overburden.

Pressure solution in a compacting medium, however, produces a great deal more grain boundary dissolution than that envisaged by Hunter (1987, 1996). Not only are grains that project into open porosity structure partially dissolved, but so, too, are the surfaces of many grains in contact with each other, especially those orthogonal to the direction of maximum principal stress (Thompson, 1959; Tada and Siever, 1989). Pressure solution requires the presence of a film of fluid between grains in contact in order to accomplish such wholesale grain dissolution (Weyl, 1959). In the case of gabbroic cumulates, this would be melt. The mechanism also requires a significant overburden, which causes overpressure and drives fluid (melt) along energetically susceptible grain boundaries. Indeed, pressure solution cannot operate without it. Textural evidence for pressure solution thus is mutual interpenetration of mineral grains, one into another, sometimes in the form of microstylolites. Examples for the case of Hole 735B gabbros are shown in Fig. 11B and C. Grain flattening, leading to an appearance of preferred planar orientation of mineral grains, these having sutured borders (Skolnick, 1965; Houseknecht 1987) is an extension of this process. This has been termed 'fitted fabric' texture (Buxton and Sibley, 1981). Examples are shown in Fig. 11D and E. Evidence for thin grain-boundary melt films includes narrow and irregular, but optically continuous, bands of orthopyroxene along sutured boundaries between olivine, clinopyroxene and plagioclase (Fig. 11F and G).

Pressure solution also occurs in metamorphic rocks. An obvious form of this is when it causes volume decrease orthogonally to the direction of maximum principal stress, such as above and below hard objects like porphyroclasts, with consequent pressure growth occurring adjacent to the objects especially in the direction of least principal stress (Durney, 1976). An example is shown in Fig. 15H. In this case, the pressure-growth minerals are the oxide minerals, ilmenite and magnetite, rather than, for example, the fibrous amphibole or chlorite of a metamorphic rock. Pressure-growth thus occurred at temperatures of igneous crystallization of oxide minerals; it was not a subsolidus phenomenon. As for textural equilibrium, it is particularly prevalent in gneissic and porphyroclastic rocks, especially in folia of strongly recrystallized plagioclase which consist almost entirely of tiny neoblasts of uniform grain size, all meeting at 120° triple junctions. The epitome of porosity reduction occurs in these thin layers of highly deformed rocks.

Many olivine gabbro adcumulates of Hole 735B have strongly preferred mineral orientations, especially of plagioclase, but are not obviously deformed (Fig. 11D). This is termed *magmatic foliation* in Dick et al. (1999). However, zones of core with this texture correlate strongly in location, and especially in fabric orientation, with nearby or interleaved rock exhibiting crystal–plastic foliation (Dick et al., 2000). The literature on layered intrusions suggests several ways that this fabric may form (Meurer and Boudreau, 1998a,b). The first is that compaction can flatten randomly oriented pre-existing grains, producing a foliation but no lineation (Young and Donaldson, 1985). A variation of this is that grain flattening can result from uneven crystal growth under conditions of uniaxial stress during compaction, again producing foliation but no lineation (Maaløe, 1976). Both foliation and lineation can result from preconsolidation slumping on an inclined surface (Brothers, 1964; Higgins, 1991). Finally, traction may act on a bed of cumulates in the course of flow of viscous magma, producing both foliation and lineation (Benn and Allard, 1989; Higgins, 1991).

These are essentially all interface processes, with deformation occurring in a crystal mush beneath a large magma body. By and large, the resultant fabrics are conformable to pre-existing layering, but they can also enhance or even create the appearance of layering. The mechanism we prefer for the rocks of Hole 735B is that of pressure solution, which produces elongation of plagioclase resulting from complementary pressure growth, under conditions of shear. The fabric was produced at numerous locations

within a thick crystal pile, it is not conformable to modal and grain-size layering, which in any case is virtually absent, it crosscuts lithologic (i.e. interval) boundaries, and the dips of the fabric in the core reference frame mimic those nearby rocks with crystal–plastic deformation. In this interpretation, therefore, the plagioclases of Fig. 11E are simply a more advanced case of the alignment shown in Fig. 11D. Simple compaction was not all that expelled intergranular melt from these rocks, and reduced porosity in Hole 735B gabbros. Porosity reduction was strongly abetted by deformation.

In the context of pressure solution, the concept of 'adcumulus growth' (Morse, 1986) is somewhat of a misnomer. In sedimentary formations, significant *reduction* in thickness of beds can occur in consequence of pressure solution but occasionally leaving relics of resistant material in stratigraphically younger surroundings (Tada and Siever, 1989). The effectiveness of pressure solution also depends on the spacing of permeable grain boundaries, and this depends on mineral type, grain size, and the state of deformation (stress) of the rocks. In oxide gabbros of Hole 735B, ilmenite and magnetite may have been especially resistant to pressure solution because of their ability to anneal readily (Agar and Lloyd, 1996) and form coarse, impermeable intergrowths during deformation. Pressure solution therefore may have modified modal proportions in some gabbros by preferentially extracting silicates, particularly plagioclase, and leaving rocks consisting predominantly of ilmenite, magnetite, and clinopyroxene in nothing like cotectic proportions, and with textures resembling nothing like textural equilibrium (Fig. 11I).

Use of part or all cumulate terminology has recently been challenged in light of changing perceptions of the mechanisms of crystal growth in layered intrusions. Hunter (1998) preferred retention of the term 'cumulate', but abandonment of terms such as 'adcumulate' because they are ambiguous and model-dependent. As defined by Irvine (1982), however, adcumulate has a specific meaning with respect to porosity, and this can be quantified. Whatever the mechanism of formation of cumulates with very low residual melt porosity, a single term to designate such rocks is still useful, and the only one that has ever been proposed is adcumulate. There is no need to abandon this term altogether.

9.8. The bitter end of differentiation

The abundant oxide-bearing and oxide-rich ferrogabbros and the few trondhjemetic veins in the upper 500 m of Hole 735B formed in consequence of a strong high-iron trend of differentiation (Natland et al., 1991). The new drilling reinforces this conclusion, but provides evidence that granitic melts were persistently produced at the extreme end of differentiation in many places throughout the section. A surprise was that the several veins analyzed during Leg 176 have considerable variability in Na_2O/K_2O, thus range from trondhjemite to true granite in composition (Dick, Natland, Miller et al., 1999). There is also little doubt that these extreme differentiates are intimately associated with oxide seams, many of which are cored with silicic veinlets (e.g. Fig. 4). Future study will determine whether straightforward crystallization differentiation or perhaps liquid immiscibility, produced the granitic residua.

Whatever the mechanism, petrographic observations indicate that very late-stage differentiation occurred under hydrous conditions. Brown amphibole is a persistent mineral associated with the two oxides, ilmenite and magnetite, and with globular sulfides, in oxide-rich seams These minerals are also the most typical intergranular association in olivine gabbros and troctolites in the lower 1000 m of the core, being present from trace amounts up to a maximum of about 3% of the mode in such rocks (Fig. 12A and B). In most of theses, neither oxides nor sulfides are affected by metamorphism, thus the associated brown amphibole appears to be primary.

The minerals are not likely the in situ crystallization products of trapped melt, since there is no obvious zoning of adjacent olivines, pyroxenes and plagioclases, both oxides and sulfides are present in excess proportions within the intergranular patches, and the patches contain no plagioclase. Instead, the components of the minerals appear to have crystallized from melt injected into fine-scale porosity structure within the more primitive host cumulates, even to the extent of ilmenite rimming spinel and occurring in cracks within olivine (Fig. 12C–E). Symplectic intergrowth of ilmenite into pyroxene at grain boundaries also occurs (Fig. 12F). This is Bowen's 'discontinuous crystallization' observed at the scale of mineral grains. Earlier, from geochemistry, we argued that the

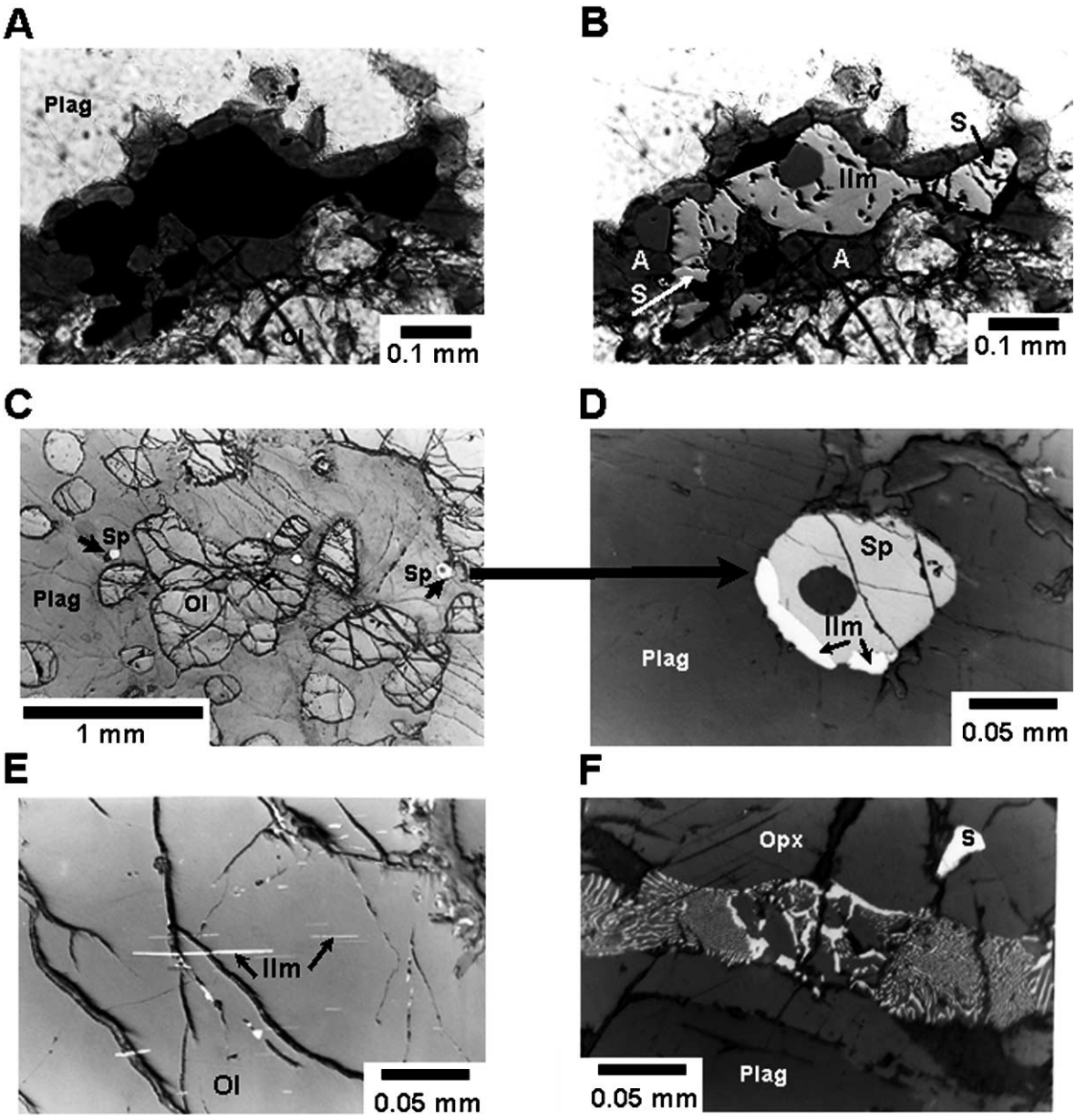

Fig. 12. Photomicrographs of the intergranular mineral assemblage in olivine gabbros of olivine gabbros and troctolites of Hole 735B. (A and B) Sample 176-735B-94R-3, 119–121 cm. Intergrown ilmenite (ilm) and sulfides (S) surrounded by brown amphibole (A) between plagioclase (plag) and olivine (ol). A is in transmitted light, B in combined transmitted and reflected light. (C and D) Sample 176-735B-91R-5, 105–107 cm. In C, a reflected light photomicrograph showing olivine (ol), with prominent cracks and high relief, and Cr-spinel (sp; white), both set in plagioclase (plag). D is a high-magnification reflected-light photomicrograph of the spinel on the right edge of C, showing an ilmenite rim (ilm) on the spinel. (E) Sample 176-735B-158R-5, 135–141 cm. Ilmenite along parting in olivine. Reflected-light photomicrograph. (F) Sample 176-735B-153R-2, 24–28 cm. Complex ilmenite-orthopyroxene (opx) symplectite in reflected light. Other minerals are plagioclase (Plag) and sulfide (S).

composition of melt 'finally trapped' in these gabbros was not basaltic. In most cases, petrography indicates that it was at least an extremely differentiated and hydrous melt, exceptionally enriched in both iron and titanium, and saturated in sulfide. The path from there to granitic melts is still uncharted, but there is as yet no indication that comparatively anhydrous ferrogranophyres of the type found at Skaergaard, in which olivines attain compositions of nearly pure fayalite (Wager and Deer, 1939; Wager and Brown, 1967), exist in this body of the lower ocean crust.

10. Comparisons with ophiolites

Is there a counterpart to the section drilled at Hole 735B among those vestiges of ocean crust called ophiolites? As with the concept of magma chambers in the ocean crust, there is a notion of ophiolites that has shifted through time. Instead of tying pillows, sheeted dikes, gabbros and ultramafic cumulates to one simple, repetitively injected and tapped magma chamber at a spreading ridge, we now recognize that ophiolites represent composite intrusions, and that they experienced complicated patterns of injection of dikes and sills, deformation, and post-cumulus re-equilibration throughout the lower crust. In this conceptual milieu, does the first detailed look at an actual section of the lower crust in an ocean basin provide new insights?

One perception derived mainly from ophiolites is that gabbro cumulates should become generally more primitive downward, and give way to ultramafic cumulates just above the mantle (e.g. Moores and Vine, 1971; Irvine and Findlay 1972; Greenbaum, 1972; Coleman, 1977; Casey et al., 1981; Pallister and Hopson, 1981; Fox and Stroup, 1982). Although Hole 735B did not reach the upper mantle, this is not the pattern of the rocks so far drilled at the site. The most primitive rocks, in fact, are from the upper third of the hole, and there are several repetitions of an underlying, fundamental cryptic variation among olivine gabbros and troctolites. These suggest either that there were several principal pulses of magma during a sustained period of crustal growth, or that deformation produced internal changes in permeability of a crystal mush, which originally may have been interconnected from top to bottom, that effectively isolated each pluton into separate differentiating entities. Later on, however, a new network of narrow fractures and shear zones reconnected the nested plutons, and late differentiates ramified through the entire body of rock, although they tended to concentrate in the upper part of the section. This particular sequence, and the resultant distribution of primitive and highly differentiated rocks, has not yet been described from any ophiolite.

The pattern of deformation is also different from that of intact ophiolites, such as Troodos, Oman, and Bay of Islands, for a very good reason. Wherever a sequence of pillows and sheeted dikes directly overlies gabbro, in the ocean crust or in an ophiolite, there has not been detachment *at that level in the crust*. Thus although small zones of crystal–plastic deformation may occur at high levels in these ophiolites, the prominence of deformation at Hole 735B is tied to the unroofing of the section — the partitioning of pillows and dikes from gabbros and ultramafic rocks, and their physical separation in opposite directions by hundreds of kilometers during seafloor spreading. It stands to reason that if the gabbros in an ophiolite are still roofed at least by dikes, they will not exhibit the strong link between deformation and the later stages of differentiation seen at Hole 735B. There may be crosscutting oxide gabbros and granitoid veinlets in such ophiolites, but they tend mainly to be hosted by allied, strongly differentiated gabbros, such as gabbronorites, and they are not strongly deformed (e.g. Bay of Islands; Bédard, 1991, 1993). At Oman, structurally high gabbros have an originally vertical magmatic foliation, but this was produced during intrusion of a crystal mush, and is not associated with dipping crystal–plastic deformation (MacLeod and Yaouancq, 2000).

At the North Arm massif of Bay of Islands, porphyroclastic and gneissic rocks occur in ultramafic cumulates near the base of the plutonic section. Bédard and Hébert (1996) believe that they were produced by shear imparted by tectonized residual peridotite as it turned over from a predominantly vertical pattern of flow during ascent beneath the ridge, to horizontal flow on the ridge flanks. At Oman, however, strong crystal–plastic fabrics are not preserved in the deepest gabbroic rocks (e.g.

Reuber, 1991). Instead, the base of the Abyad section (MacLeod and Yaouancq, 2000) consists of a layered sequence some 1500 m thick that is now understood largely to represent intrusion of sills into a crystal mush by primitive magma (Boudier et al., 1996; Kelemen et al., 1997; Kelemen and Aharonov, 1999). Deformation does not completely obscure a similar phenomenon at North Arm Mountain, Bay of Islands (Bédard, 1993).

There is no sign of similar sill implacement in the gabbros of Hole 735B. Indeed, evidence of vertical injection of magma is more pronounced in the deepest pluton than anywhere else in the core. Discounting deformation, the entire 1.5 km section can be described broadly as varitextured. At Oman, similar rocks are only about 200 m thick, they are at the very top of the section, and they are the only place where oxide gabbros, exclusively in the form of pegmatites, occur (e.g. MacLeod and Yaouancq, 2000). At North Arm, similar rocks are termed 'isotropic', and they, too, are restricted to the top of the section, and overlie layered gabbros (Bédard, 1991). If a strongly layered plutonic sill sequence exists an Atlantis Bank, it underlies Hole 735B, or is out of the section altogether. At Oman, the phenomenon may be tied to a high spreading rate and the existence of a wide mass of soft crystal mush (Kelemen et al., 1997), in which case what has been seen so far at Hole 735B will not change with depth.

Since the initial drilling of Hole 735B, rocks with generally similar attributes have been described from the Lizard ophiolite in Cornwall (Hopkinson and Roberts, 1995), and ophiolite remnants of the Western and Ligurian Alps (Caby, 1995; Molli, 1995). These have the advantage over Troodos, Bay of Islands, and Oman in genuinely having MORB, rather than 'supra-subduction' geochemical and mineralogical attributes. The most important similarity to Hole 735B is association of strikingly oxide-rich ferrogabbros with zones of strong crystal–plastic deformation. The oxide gabbros crosscut more primitive gabbros, which in turn intrude, or are in fault contact with, deformed peridotite. Basalts and dikes are at best only minor components of these remnants. Systematic relationships through a long sequence of gabbros have not yet been established at any of these ophiolites, but it is tempting to speculate that they are the lopped off tops of high transverse ridges that formed adjacent to transform faults of ancient slowly spreading ridges.

11. Comparisons with layered intrusions

We have concentrated on demonstrating dissimilarities between the section at Hole 735B, and the processes that produced it, with those layered intrusions for which modern interpretation still requires crystallization from large bodies or sheets of magma, either injected as voluminous single pulses, or sustained by re-injection over long periods of time. Both classical and modern cumulate theory derives from study of such intrusions. The conceptual dimensions of these magma bodies may have diminished over the last decades of research, but they have not disappeared. Beneath these magma bodies, crystal mushes are considered to have been thicker than first imagined, and post-cumulus compaction and textural re-equilibration to act in them further from magma-chamber floors. However, the general conceptual arrangement of crystalline segregations and a large magma body in cumulate theory is intact.

Hole 735B, however, requires formulation of cumulate theory, and consideration of almost all cumulus processes, including primary precipitation of minerals, compaction, textural re-equilibration, and porosity reduction, in the absence of even a small, sustained magma chamber. The action was consistently in narrow zones of magma injection and re-injection, at most a few meters wide, but of times much smaller. The distribution of these zones was determined by a combination of fluctuating magma supply, crustal dilatancy (spreading), oblique faulting, and shear. The interactive mass of cumulates and magma spanned the entire thickness of the gabbroic layer. Lateral intrusion of picritic magma into crystal mushes, a common feature of ophiolites and layered intrusions, did not occur in the rocks drilled at Hole 735B, and has not yet been demonstrated anywhere else in the ocean crust. Upward migration of magma to form a single melt lens of the type visualized for fast-spreading ridges did not occur; it was at least partially thwarted by the complexity of the overlying stratigraphy, and by simultaneous deformation. Infiltrative mixing, metasomatism, and reaction with surrounding rocks (Bédard and Hebert, 1996)

influenced all stages of the liquid line of descent (Natland et al., 1991; Dick et al., 1991a; Dick et al., 2000).

Of the major layered intrusions featured in Cawthorn's (1996) recent compendium, the Duluth Complex offers the strongest comparisons to Hole 735B. This may be because it also formed beneath a rift valley. Different structural levels are exposed, and the Complex is probably best described as an aggregate of intrusions. Some of these are large bodies that evidently crystallized from single, large pulses of magma, resulting in a regular progressive cryptic variation with stratigraphic height (e.g. the Sonju Lake Intrusion; Miller and Chandler, 1997). The Partridge River Intrusion, on the other hand, matches Hole 735B in the vertical scale and range of lithologic variability (Severson, 1991). The origin of the fluctuations in composition is controversial. They are interpreted either to be a consequence of retention of different, but high, proportions of trapped melt (Chalokwu and Grant, 1990; Chalokwu et al., 1993), or repetitive injections of magma (Miller and Ripley, 1996), together with variable reaction between magma and xenoliths of iron-rich sedimentary rock (Severson and Hauck, 1990; Severson, 1991). A 600 m drill core from the South Kiwashiwi intrusion consists of seven principal units of texturally variable troctolite and olivine gabbro, with lesser melanocratic gabbro and norite (Miller and Ripley, 1996). One troctolite unit contains local oxide-rich layers. The units are remniniscent of the stacked plutons of Hole 735B. However, Lee and Ripley (1996) model the sequence by in situ crystallization coupled with magma recharge and expulsion of intercumulus melt into a main magma reservoir following each recharge cycle. In contrast to gabbros of Hole 735B, these rocks are described as having some non-cumulate textural features, and bulk compositions indicating retention of significant fractions of trapped basaltic melt (Chalokwu and Grant, 1990).

Anorthosites comprise about 35–40% of the Duluth Complex (Miller and Weiblein, 1990). Although they have strong plagioclase alignment, they are not layered. Crosscutting contact relationships and patterns of poikilitic crystal growth indicate that they formed by multiple intrusions of crystal mushes. In these respects they resemble the least deformed olivine gabbros of Hole 735B. Nevertheless, they have no crystal–plastic deformation.

Some layered intrusions have late discordant gabbroic or melagabbroic pipes rich in iron–titanium oxides that crosscut primitive cumulates. Those of the Partridge River Intrusion of the Duluth complex are described only from drill cores (Severson and Hauck, 1990; Severson, 1991). Where they originated in the intrusion, or even if they originated in the same mass of crystallizing rock, which has a complex underlying igneous stratigraphy, are uncertain. In the Bushveld Complex, the composition of discordant oxide gabbros is related to height in the formation (Viljoen and Scoon, 1985; Scoon and Mitchell, 1994), although individually they are described as precipitates from pools of dense, iron-rich magmas (Bateman, 1951; Reynolds, 1985), some of which sank into underlying unconsolidated cumulates in pipe-like fashion only to reach less permeable layers above which they penetrated sideways, in the manner of sills (Scoon and Mitchell, 1994). At Hole 735B, however, melt densities were insufficient to allow iron-rich magmas to sink into cumulates composed of silicate minerals and a small percentage of intercumulus liquid. Rather, buoyant magmas rose, although they may well have penetrated the formation sideways *beneath* impermeable horizons that they later breached. At both Bushveld and Hole 735B, oxide minerals concentrated in porosity structure as differentiated, iron-rich magma flowed through it, and the resultant ferrogabbros in both cases are a type of cumulate, albeit not one that formed on the floor of a magma chamber.

12. Comparison with emplacement of granitic plutons in continental crust

Emplacement of granite plutons provides possible analogs to the combination of magmatism and deformation seen in the gabbros of Hole 735B. Many granite plutons exhibit deformation fabrics at their margins related to shear that were produced during emplacement of partly molten crystal mushes in various tectonic regimes (Pitcher, 1993). Hutton (1988) related particular granite deformation fabrics

to the state of crystallization of the magma, distinguishing deformation prior to full crystallization in the rocks from deformation producing crystal–plastic strain. He emphasized that shear might well occur before the crystal-laden system 'locks-up', and thus be very difficult to recognize; the rocks will appear to be undeformed even having experienced a history of shear. Perhaps of most pertinence to Hole 735B is the situation of diapiric uprise intercepting intra-crustal listric extensional faults or shear zones leading to formation of listric sheets. A combination of diapiric uprise, shear deformation and cooling provides a mechanism for the development of compositionally zoned plutons, and upward-increasing extent of differentiation in inclined sheets. Bearing in mind the difficulties of inferring large-scale structural features from a single long core only 6 cm in diameter, we surmise that the separate 'plutons' of Hole 735B could be balloon-like intrusions, reminiscent of the simplest of magma chambers, but now stretched into separate, upwardly differentiated sheets by the deformation that accompanied unroofing and uplift of the entire section. These probably would not be detectable at all without the detailed sampling carried out during Legs 118 and 176. Continued congelation and differentiation of basaltic magma allowed development of fabrics of crystal–plastic strain, when perhaps 30% of melt remained in the rocks (Hutton, 1988, Fig. 2). Thereafter, all of the late-stage crosscutting oxide gabbros and felsic veins coursed through the section.

13. Conclusions

Hole 735B provides a first indication of the importance of synkinematic igneous differentiation (Dick et al., 1991b), also termed differentiation by deformation (Bowen, 1920), in the ocean crust. It allows a comprehensive assessment of this process wherein shallow gabbros, occurring in the form of small, nested plutons, were enriched in late iron-rich melt derived from a collection of plutons by means of compaction (or filter-pressing) and tectonic processes, rather than simple gravitationally-driven crystallization differentiation. High-temperature metamorphic and deformational processes continued into the subsolidus, followed by lower-temperature brittle fracturing, metamorphism and alteration, but at this stage with little attendant deformation of the uplifting mass of plutonic rocks. This accounts for the persistence of magnetic anomalies across Atlantis Bank, and may explain why there are magnetic anomalies at all along slowly spreading ridges. Hole 735B allows us to assess these complexly interactive processes in a known tectonic setting, at a ridge of established rate spreading rate and topography. It is, and it is likely to remain, the standard section for a slowly spreading ridge, whether it is explored elsewhere in the ocean crust, or in an ophiolite.

Acknowledgements

Thanks to the crew and drillers of JOIDES Resolution, and the technical staff of both Legs 118 and 176 for being so strongly 'with it' as the cores of 'grabbro', so different from subtly multi-hued, but basically dull green, marine sediment cored during prior and following legs, came on board. Rock saws, sticky glue, tiny labels, sample parties, and computer sustenance at sea are all essential parts of this study. Particular thanks to thin section specialists Joe Powers and Ted Gustafson, and XRF specialists Wendy Autio and Don Sims, whose work provided so much of the data discussed here. The work of the scientific parties of both Legs 118 and 176, of course, was absolutely essential to the acquisition of most of the data discussed here. They were also strongly involved in the development and discussion of many of the ideas presented here, although few of the shipboard scientists would agree with everything we have said. Bill Meurer and Jean Bédard thoughtfully reviewed the paper. Finally, thanks to Kevin Burke, who seems to know everything, for recalling Alfred Harker.

References

Agar, S.M., Lloyd, G.E., 1996. Deformation of Fe–Ti oxides in gabbroic shear zones from the MARK area 1997. In: Karson, J.A., Cannat, M., Miller, D.J., Elthon, D. (Eds.), Proc. ODP, Sci. Res., vol. 153. Ocean Drilling Program, College Station, TX, pp. 123–141.

Allan, J.F., 1993. Cr-spinel as a petrogenetic indicator: deducing magma composition from spinels in highly altered basalts from

the Japan Sea, Sites 794 and 797. In: Tamaki, K., Suyehiro, K., Allan, J., McWilliams, M., Proc. ODP, Sci. Results Part 2, vol. 127/128. Ocean Drilling Program, College Station, TX, pp. 837–847.

Allan, J.F., Sack, R.O., Batiza, 1988. Cr-spinels as petrogenetic indicators: MORB-type lavas from the Lamont Seamount Chain, eastern Pacific. Am. Mineral. 73, 741–753.

Anderson, A.T., Greenland, L.P., 1970. Phosphorus fractionation diagram as a quantitative indicator of crystallization differentiation of basaltic liquids. Geochim. Cosmochim. Acta 33, 493–505.

Aumento, F., Melson, W.G., et al., 1974. Init. Rep. DSDP, 37. U.S. Government Printing Office, Washington.

Barrow, J., 1892. On certain gneisses with round-grained oligoclase and their relation to pegmatites. Geol. Mag., Decade 3 (9), 64–65.

Barrow, J., 1893. On an intrusion of muscovite–biotite gneiss in the southeastern highlands of Scotland, and its accompanying metamorphism. Q. J. Geol. Soc. 49, 330–356.

Bateman, A.M., 1951. The formation of late magmatic oxide ores. Econ. Geol. 46, 404–426.

Bédard, J., 1991. Cumulate recycling and crustal evolution in the Bay of Islands ophiolite. J. Geol. 99, 225–249.

Bédard, J., 1993. Oceanic crust as a reactive filter: synkinematic intrusion, hybridization, and assimilation in an ophiolitic magma chamber, western Newfoundland. Geology 21, 77–80.

Bédard, J., 1994. A procedure for calculating the equilibrium distribution of trace elements among the minerals of cumulate rocks, and the concentration of trace elements in coexisting liquids. Chem. Geol. 118, 143–153.

Bédard, J., Hébert, R., 1996. The lower crust of the Bay of Islands ophiolite, Canada: petrology, mineralogy, and the importance of syntexis in magmatic differentiation in ophiolites and at ocean ridges. J. Geophys. Res. 101, 25105–25124.

Bédard, J., Sparks, R.S.J., Renner, R., Cheadle, M.J., Hallworth, M.A., 1988. Peridotite sills and metasomatic gabbros in the eastern layered series of the Rhum complex. J. Geol. Soc. 145, 207–224.

Benn, K., Allard, B., 1989. Preferred mineral orientations related to magnatic flow in ophiolite layered gabbros. J. Petrol. 30, 925–946.

Bloomer, S.H., Meyer, P.S., Dick, H.J.B., Ozawa, K., Natland, J.H., et al., 1991. Textural and mineralogic variations in gabbroic rocks from Hole 735B. In: Von Herzen, R.P., Robinson, P.T., et al., Proc. ODP, Sci. Results, 118. , pp. 21–39.

Boudier, F., Nicolas, A., Ildefonse, B., 1996. Magma chambers in the Oman ophiolite: fed from the top and the bottom. Earth Planet. Sci. Lett. 144, 239–250.

Bowen, N.L., 1920. Differentiation by deformation. Proc. Natl. Acad. Sci. 6, 159–162.

Brothers, R.N., 1964. Petrofabric analyses of Rhum and Skaergaard layered rocks. J. Petrol. 5, 255–274.

Brown, G.M., 1956. The layered ultrabasic rocks of Rhum, Inner Hebrides. Philos. Trans. R. Soc. London B 240, 1–53.

Bryan, W.B., Moore, J.G., 1977. Compositional variations of young basalts in the Mid-Atlantic Ridge rift valley near lat 36°49′N. Geol. Soc. Am. Bull. 88, 556–570.

Buxton, T.M., Sibley, D.F., 1981. Pressure solution features in a shallow buried limestone. J. Sediment Petrol. 51, 19–26.

Caby, R., 1995. Plastic deformation of gabbros in a slow-spreading Mesozoic ridge: example of the Montgenèvre ophiolite, western Alps. In: Vissers, R.L.M., Nicolas, A. (Eds.), Mantle and Lower Crust Exposed in Oceanic Ridges and in Ophiolites. Kluwer Academic Publishers, Dordrecht, pp. 123–145.

Campbell, I.H., 1996. Fluid dynamic processes in basaltic magma chambers. In: Cawthorn, R.G. (Ed.), Layered Intrusions. Elsevier, Amsterdam, pp. 45–76.

Cann, J.R., 1974. A model for oceanic crustal structure developed. Geophys. J. R. Astron. Soc. 39, 169–187.

Cann, J.R., Blackman, D.K., Smith, D.K., McAllister, E., Janssen, B., Mello, S., Avgerinos, E., Pascoe, A.R., Escartin, J., 1997. Corrugated slip surfaces formed at ridge-transform intersections on the Mid-Atlantic Ridge. Nature 385, 329–332.

Cannat, M., 1991. Plastic deformation at an oceanic spreading ridge: a microstructural study of Site 735 gabbros (Southwest Indian Ocean). In: Von Herzen, R.P., Robinson, P.T., et al., Proc. ODP, Sci. Results, vol. 118. Ocean Drilling Program, College Station, TX, pp. 399–408.

Cannat, M., 1993. Emplacement of mantle rocks in the seafloor at mid-ocean ridges. J. Geophys. Res. 98, 4163–4172.

Cannat, M., Mével, C., Stakes, D., et al., 1991. Normal ductile shear zones at an oceanic spreading ridge: tectonic evolution of Site 735 gabbros (Southwest Indian Ocean). In: Von Herzen, R.P., Robinson, P.T., et al. (Eds.), Proc. ODP, Sci. Results, vol. 118. Ocean Drilling Program, College Station, TX, pp. 415–429.

Casey, J.F., Dewey, J.F., Fox, P.J., Karson, J.A., Rosencrantz, E., 1981. Heterogeneous nature of oceanic crust and upper mantle: a perspective from the Bay of Islands Ophiolite Complex. In Emiliani, C., The Sea (Vol. 7): The Oceanic Lithosphere: New York (Wiley), 305–338.

Cawthorn, R.G. (Ed.), 1996. Layered Intrusions. Elsevier, Amsterdam.

Chalokwu, C.I., Grant, N.K., 1990. Petrology of the Partridge River intrusion, Duluth Complex, Minnesota: I. Relationships between mineral compositions, density, and trapped liquid abundance . J. Petrol. 31, 265–293.

Chalokwu, C.I., Grant, N.K., Ariskin, A.A., Birmana, G.S., 1993. Simulation of primary phase relations and mineral compositions in the Partridge River intrusion, Duluth Complex, Minnesota: implications for the parent magma composition. Contrib. Mineral. Petrol. 114, 539–549.

Clague, D.A., Frey, F.A., Thompson, G., Rindge, S., 1981. Minor and trace element geochemistry of volcanic rocks dredged from the Galapagos Spreading Center: role of crystal fractionation and mantle heterogeneity. J. Geophys. Res. 86, 9469–9482.

Coleman, R.G., 1977. Ophiolites. Springer, Berlin.

Crawford, W.C., Webb, S.C., Hildebrand, J.A., 1999. Constraints on melt in the lower crust and Moho at the East Pacific Rise, 9°48′N, using seafloor compliance measurements. J. Geophys. Res. 104, 2923–2939.

Daly, R.A., 1933. Igneous Rocks and the Depths of the Earth. Hafner, New York (Reprint, 1968).

DeLong, S.E., Chatelain, C., 1990. Trace-element constraints on

accessory-phase saturation in evolved MORB magma. Earth Planet. Sci. Lett. 101, 206–215.

Dick, H.J.B., 1989. Abyssal peridotites, very slow spreading ridges and ocean ridge magmatism. In: Magmatism in the Ocean Basins, Saunders, A.D., Norry, M.J. (Eds.). Geol. Soc. Spec. Publ. 42, 71–105.

Dick, H.J.B., Schouten, H., Meyer, P.S., Gallo, D.G., Bergh, H., Tyce, R., Patriat, P., Johnson, K.T.M., Snow, J., et al., 1991a. Tectonic evolution of the Atlantis II Fracture Zone. In: Von Herzen, R.P., Robinson, P.T., et al., Proc. ODP, Sci. Results, 118. Ocean Drilling Program, College Station, TX, pp. 439–538.

Dick, H.J.B., Meyer, P.S., Bloomer, S., Kirby, S., Stakes, D., Mawer, C., et al., 1991b. Lithostratigraphic evolution of an in-situ section of oceanic layer 3. In: Von Herzen, R.P., Robinson, P.T., et al., Proc. ODP, Sci. Results, 118. Ocean Drilling Program, College Station, TX, pp. 439–538.

Dick, H.J.B., MacLeod, C.J., Robinson, P.T., Allerton, S., Tivey, M., James Clark Ross 31 Scientific Party, 1999a. Bathymetric Map of the Atlantis Bank Platform. In: Dick, H.J.B., Natland, J.H., Miller, D.J., et al., Proc. ODP, Init. Rep., vol. 176. Ocean Drilling Program, College Station, TX (back pocket illustration).

Dick, H.J.B., Natland, J.H., Miller, D.J., et al., 1999b. Proc. ODP, Init. Rep., 176, Ocean Drilling Program, College Station, TX.

Dick, H.J.B., Natland, J.H., Kinoshita, Robinson, P., MacLeod, C., Kvasness, A.J., the MODE '98, JR 31, ODP Leg 176 Scientific Parties, 1999c. The nature of intrusion and melt transport in the lower ocean crust at an ultra-slow spreading ridge. Ninth Annual V.M. Goldschmidt Conference, Cambridge, Massachusetts, August 22–27, 1999, LPI Contrib. vol. 971, Lunar and Planetary Science Institute, Houston, TX, pp. 71–72.

Dick, H.J.B., Natland, J.H., Alt, J.C., Bach, W., Bideau, D., Gee, J.S., Haggas, S., Hertogen, J.G.H., Hirth, G., Holm, P.M., Ildefonse, B., Iturrino, G.J., John, B.E., Kelley, D.S., Kikawa, E., Kingdon, A., LeRoux, P.J., Maeda, J., Meyer, P.S., Miller, D.J., Naslund, H.R., Niu, Y-L., Robinson, P.T., Snow, J., Stephen, R.A., Trimby, P.W., Worm, H.-U., Yoshinobu, A., 2000. A long in situ section of the lower ocean crust: results of ODP Leg 176 drilling at the Southwest Indian Ridge. Earth Planet. Sci. Lett. 179, 31–51.

Dixon, S., Rutherford, M.J., 1979. Plagiogranites and late-stage immiscible liquids in ophiolites and mid-ocean ridge suites: an experimental study. Earth Planet. Sci. Lett. 45, 45–60.

Dmitriev, L., Heirtzler, J., et al., 1979. Init. Rep. DSDP, 46. US Government Printing Office, Washington.

Dungan, M.A., Rhodes, J.M., 1978. Residual glasses and melt inclusions in basalts from DSDP Legs 45 and 46: evidence for magma mixing. Contrib. Mineral. Petrol. 67, 417–431.

Durney, D.W., 1976. Pressure-solution and crystallization deformation. Philos. Trans. R. Soc. Lond. A 283, 229–240.

Eales, H.V., Cawthorn, R.G., 1996. The Bushveld Complex. In: Cawthorn, R.G. (Ed.), Layered Intrusions. Amsterdam, Elsevier, pp. 181–229.

Emeleus, C.H., Cheadle, M.J., Hunter, R.H., Upton, B.G.J., Wadsworth, W.J., 1996. The Rum layered suite. In: Cawthorn, R.G. (Ed.), Layered Intrusions. Elsevier, Amsterdam, pp. 403–439.

Engel, C.G., Fisher, R.L., 1975. Granitic to ultramafic rock complexes of the Indian Ocean Ridge system, western Indian Ocean. Geol. Soc. Am. Bull. 86, 553–1578.

Fisher, R.L., Goodwillie, A., 1997. The physiography of the Southwest Indian Ridge. Mar. Geophys. Res. 19, 451–455.

Fisher, R.L., Sclater, J.G., 1983. Tectonic evolution of the Southwest Indian Ocean since the Mid-Cretaceous: plate motions and stability of the pole of Antarctica/Africa for at least 80 Myr. Geophys. J. R. Astron. Soc. 73, 553–576.

Fisher, R.L., Dick, H.J.B., Natland, J.H., Meyer, P.T., 1986. Mafic/ultramafic suites of the slowly spreading Southwest Indian Ridge: Protea exploration of the Antarctic Plate Boundary, 24°–47°E. Ofioliti 11, 147–178.

Flower, M.J.F., Robinson, P.T., 1979. Evolution of the 'FAMOUS' ocean ridge segment: evidence from submersible and deep-sea drilling investigations. In: Talwani, M., Harrison, C.G., Hayes, D.E. (Eds.), Deep Drilling Results in the Atlantic Ocean: Ocean Crust (Maurice Ewing Series 2). American Geophysics Union, Washington, pp. 314–330.

Fox, P.J., Stroup, J.B., 1982. The plutonic foundation of the oceanic crust. In: Emiliani, C., et al. (Eds.), The Sea, Part 2, vol. 4. Wiley, New York, pp. 119–218.

Greenbaum, D., 1972. Magmatic processes at ocean ridges: evidence from the Troodos massif, Cyprus. Nature Phys. Sci. 238, 18–21.

Hall, J.M., 1979. In: Talwani, M., Harrison, C.G., Hayes, D.E. (Eds.). A model for the structural state of the upper half kilometer of North Atlantic Oceanic Layer 1. Deep Drilling Results in the Atlantic Ocean: Ocean Crust (Maurice Ewing Series 2)American Geophysics Union, Washington, pp. 166–168.

Harker, A., 1904. The Tertiary Igneous rocks of Skye. Mem. Geol. Surv. UK.

Harker, A., 1909. A Natural History of the Igneous Rocks. Hafner, New York (Reprint, 1965).

Hart, S.R., Blusztain, J., Dick, H.J.B., Meyer, P.S., Muehlenbachs, K., 1999. The fingerprint of seawater circulation in a 500-meter section of ocean crust gabbros. Geochim. Cosmochim. Acta 63, 4059–4080.

Hébert, R., Constantin, M., Robinson, P.T., et al., 1991. Primary mineralogy of Leg 118 gabbroic rocks and their place in the spectrum of oceanic mafic igneous rocks. In: Von Herzen, R.P., Robinson, P.T., et al. (Eds.). Proc. ODP, Sci. Results, 118. pp. 3–20.

Higgins, M.D., 1991. The origin of laminated and massive anorthosite, Sept Isles layered intrusion, Quebec, Canada. Contrib. Mineral. Petrol. 106, 340–354.

Hopkinson, L., Roberts, S., 1995. Ridge axis deformation and coeval melt migration within layer 3 gabbros: evidence from the Lizard Complex, UK. Contrib. Mineral. Petrol. 121, 126–138.

Houseknecht, D.W., 1987. Intergranular pressure solution in four quartzose sandstones. J. Sedim. Petrol. 58, 228–246.

Hunter, R.H., 1987. Textural equilibrium in layered igneous rocks. In: Parsons, I. (Ed.). Origins of Igneous Layering. D. Reidel, Dordrecht, pp. 473–503.

Hunter, R.H., 1998. Textural development in cumulate rocks. In: Cawthorn, R.G. (Ed.). Layered Intrusions. Elsevier, Amsterdam, pp. 77–101.

Hutton, D.H.W., 1988. Granite emplacement mechanisms and tectonic controls: inferences from deformation studies. Trans. R. Soc. Edinb: Earth Sci. 79, 245–255.

Irvine, T.N., 1982. Terminology for layered intrusions. J. Petrol. 23, 127–162.

Irvine, T.N., Findlay, T.C., 1972. Alpine-type peridotite with particular reference to the Bay of Islands complex. Pub. Earth Phys. Branch Dept. Energy, Mines, Res. Can. 42, 97–128.

Irvine, T.N., Anderson, J.C.Ø., Brooks, C.K., 1998. Included blocks (and blocks within blocks) in the Skaergaard intrusion: geologic relations and the origins of rhythmic modally graded layers. Geol. Soc. Am. Bull. 110, 1398–1447.

Itturino, G., Christensen, N.I., Kirby, S., Salisbury, M.H., et al., 1991. Seismic velocities and elastic properties of oceanic gabbroic rocks from Hole 735B. In: Von Herzen, R.P., Robinson, P.T., et al., Proc. ODP, Sci. Results, 118. Ocean Drilling Program, College Station, TX, pp. 227–244.

Jackson, E.D., 1961. Primary textures and mineral associations in the ultramafic zone of the Stillwater Complex, Montana. Geol. Surv. Prof. Pap. 358.

Juster, T., Grove, T.L., Perfit, M.R., 1989. Experimental constraints on the generation of FeTi basalts, andesites and rhyodacites at the Galapagos Spreading Center, 85°W and 95°W. J. Geophys. Res. 94, 9247–9251.

Karson, J.A., 1998. Internal structure of oceanic lithosphere: a perspective from tectonic windows. Faulting and Magmatism and Mid-Ocean Ridges, Buck, W.R., Delaney, P.T., Karson, J.A., Labagrielle, Y. (Eds.). Geophys. Monogr. 106, 177–218.

Kelemen, P.B., Aharonov, E., 1999. Periodic formation of magma fractures and generation of layered gabbros in the lower crust beneath oceanic spreading centers. Faulting and Magmatism at Mid-Ocean Ridges, Buck, R., Delaney, P.T., Karson, J.A., Lagabrielle, Y. (Eds.). Geophys. Monogr. 106, 267–289.

Kelemen, P.B., Koga, K., Shimizu, N., 1997. Geochemistry of gabbro sills in the crust-mantle transition zone of the Oman Ophiolite: implications for the origin of the oceanic lower crust. Earth Planet. Sci. Lett. 146, 475–488.

Kempton, P.D., Hawkesworth, C.J., Fowler, M., et al., 1991. Geochemistry and isotopic composition of sulfur in layuer 3 gabbros from the Indian Ocean, Hole 735B. In: Von Herzen, R.P., Robinson, P.T., et al., Proc. ODP, Sci. Results, 118. Ocean Drilling Program, College Station, TX, pp. 127–143.

Kent, G.M., Harding, A.J., Orcutt, J.A., 1993. Distribution of magma beneath the East Pacific Rise between the Clipperton Transform and the 9°17′N Deval from forward modeling of commong depth point data. J. Geophys. Res. 98, 13,945–13,969.

Kikawa, E., Pariso, J., et al., 1991. Magnetic properties of gabbros from Hole 735B, Southwest Indian Ridge. In: Von Herzen, R.P., Robinson, P.T., et al., Proc. ODP, Sci. Results, 118. Ocean Drilling Program, College Station, TX, pp. 285–307.

Kinzler, R.J., Grove, T.M., 1993. Corrections and further discussion of the primary magmas of mid-ocean ridge basalts, 1 and 2. J. Geophys. Res. 98, 22,339–22,347.

Klein, E., Langmuir, C.H., 1987. Ocean ridge basalt chemistry, axial depth, crustal thickness, and temperature variations in the mantle. J. Geophys. Res. 92, 8089–8115.

Lagabrielle, Y., Bideau, D., Cannat, M., Karson, J.A., Mével, C., 1998. Ultramafic–mafic plutonic rock suites exposed along the Mid-Atlantic Ridge (10°N–30°N). Symmetrical–assymetrical distribution and implications for seafloor spreading processes. Faulting and Magmatism and Mid-Ocean Ridges, Buck, W.R., Delaney, P.T., Karson, J.A., Labagrielle, Y. (Eds.). Geophys. Monogr. 106, 153–176.

Lange, R., Carmichael, I.S.E., 1990. Thermodynamic properties of silicate liquids with emphasis on density, thermal expansion, and compressibility. Modern Methods of Igneous Petrology: Understanding Magmatic Processes, Nicholls, J., Russell, J.K. (Eds.). Rev. Mineral. 24, 25–64.

Lee, I., Ripley, E.M., 1996. Mineralogic and oxygen isotopic studies of open system magmatic processes in the South Kawishiwi Intrusion, Spruce Road area, Duluth Complex, Minnesota. J. Petrol. 37, 1437–1461.

Leg 176 Scientific Party, 1999. Site 735. In: Dick, H.J.B., Natland, J.H., Miller, D.J., et al., Proc. ODP, Init. Rep., vol. 176. Ocean Drilling Program, College Station, TX, pp. 1–314 (CD-ROM).

Maaløe, S., 1976. The zoned plagioclase of the Skaergaard intrusion, East Greenland. J. Petrol. 17, 398–419.

MacLeod, C.J., Yaouancq, G., 2000. A fossil melt lens in the Oman ophiolite: implications for magma chamber processes at fast spreading ridges. Earth Planet. Sci. Lett. 176, 357–373.

MacLeod, C.J., Allerton, S., Dick, H.J.B., Robinson, P.T., the JR31 Scientific Party, 1998. Geology of Atlantis Bank, SW Indian Ridge: preliminary Results of RRS James Clark Ross Cruise 31. Eos 79, Fall Meeting Supplement F893.

Marsh, B.D., 1989. Magma chambers. Annu. Rev. Earth Planet. Sci. 17, 439–474.

Marsh, B.D., 1995. Solidification fronts and magmatic evolution. Mineral. Mag. 60, 5–40.

McBirney, A.R., 1996. The Skaergaard Intrusion. In: Cawthorn, R.G. (Ed.), Layered Intrusions. Elsevier, Amsterdam, pp. 147–180.

McCallum, I.S., 1996. The Stillwater Complex. In: Cawthorn, R.G. (Ed.), Layered Intrusions. Elsevier, Amsterdam, pp. 441–484.

Melson, W.G., Rabinowitz, P.D., et al., 1979. Init. Rep. DSDP, 45. US Government Printing Office, Washington.

Meurer, W.P., Boudreau, A.E., 1998a. Compaction of igneous cumulates part I: Geochemical consequences for cumulates and liquid fractionation trends. J. Geol. 106, 281–292.

Meurer, W.P., Boudreau, A.E., 1998b. Compaction of igneous cumulates part II: Compaction and the development of igneous foliations. J. Geol. 106, 293–304.

Miller, Jr., J.D., Chandler, V.W., 1997. Geology, petrology, and tectonic significance of the Beaver Bay Complex, northeastern Minnesota. In, Ojakangas, R.W., Dickas, A.B., Green, J.C., (Eds), Mid-Proterozoic to Cambrian Rifting, Central North America. Geol. Soc. Am. Spec. Paper 312, 73–96.

Miller, Jr., J.D., Ripley, E.M., 1996. Layered intrusions of the Duluth Complex, Minnesota, USA. In: Cawthorn, R.G. (Ed.), Layered Intrusions. Elsevier, Amsterdam, pp. 257–302.

Miller, Jr, J.D., Weiblein, P.W., 1990. Anorthositic rocks of the

Duluth Comples: examples of rocks formed from plagioclase crystal mush. J. Petrol. 31, 295–339.

Minshull, T.A., White, R.S., 1996. Thin crust on the flanks of the slow spreading Southwest Indian Ridge. Geophys. J. Int. 125, 139–148.

Molli, G., 1995. Pre-orogenic high-temperature shear zones in an ophiolite complex, Bracco Massif, Northern Appenines, Italy. In: Vissers, R.L.M., Nicolas, A. (Eds.), Mantle and Lower Crust Exposed in Oceanic Ridges and in Ophiolites. Kluwer Academic Publishers, Dordrecht, pp. 147–161.

Morse, S.A., 1979. Kiglapait geochemistry I: systematics, sampling, and density. J. Petrol. 20, 555–590.

Morse, S.A., 1986. Convection in aid of adcumulus growth. J. Petrol. 27, 1183–1214.

Moores, E.M., Vine, F.J., 1971. Troodos Massif, Cyprus and other ophiolites as oceanic crust: evaluation and implications. R. Soc. Lond. Philos. Trans. A 268, 443–466.

Muller, M.R., Robinson, C.J., Minshull, R.S., Bickle, M.J., 1997. Thin crust beneath ocean drilling program borehole 735B at the Southwest Indian Ridge? Earth Planet. Sci. Lett. 148, 93–108.

Natland, J.H., 1980. Effect of axial magma chambers beneath spreading centers on the compositions of basaltic rocks. In: Rosendahl, B.R., Hékinian, R., et al., Init. Rep. DSDP, 54. US Government Printing Office, Washington, pp. 833–850.

Natland, J.H., 1991. Indian Ocean crust. In: Floyd, P.A. (Ed.), Oceanic Basalts. Glasgow, Blackie, pp. 63–93.

Natland, J.H., Dick, H.J.B., 1996. Melt migration through high-level gabbroc cumulates of the East Pacific Rise at Hess Deep: the origin of magma lenses and the deep crustal structure of fast-spreading ridges. In: Mével, C., Gillis, K.M., Allan, J.F., Meyer, P.S., Proc. ODP, Sci. Results, 147. Ocean Drilling Program, College Station, TX, pp. 21–58.

Natland, J.H., Meyer, P.S., Dick, H.J.B., Bloomer, S.H., et al., 1991. Magmatic oxides and sulfides in gabbroic rocks from Hole 735B and the later development of the liquid line of descent. In: Von Herzen, R.P., Robinson, P.T., et al., Proc. ODP, Sci. Results, 118. Ocean Drilling Program, College Station, TX, pp. 75–111.

Nisbet, E.G., Fowler, C.M.R., 1978. The Mid-Atlantic Ridge at 37° and 45°N: some geophysical and petrological constraints. J. R. Astron. Soc. 45, 631–660.

Niu, Y.-L., 1991. Batiza In situ densitiers of MORB melts and residual mantle: Imp;lications for buoyancy forces beneath mid-ocean ridges. J. Geol. 99, 767–775.

O'Hara, M.J., 1977. The geochemistry of lavas erupted from a magma chamber undergoing fractional crystallization with periodic addition and intermingling of more primitive magma. Nature 266, 503–507.

O'Hara, M.J., Mathews, R.E., 1981. Geochemical evolution in an advancing, periodically replenished, periodically tapped, continuously fractionating magma chamber. J. Geol. Soc. 138, 237–277.

Ozawa, K., Meyer, P.S., Bloomer, S.H., et al., 1991. Mineralogy and textures of iron–titanium oxide gabbros and associated olivine gabbros from Hole 735B. In: Von Herzen, R.P., Robinson, P.T., et al., Proc. ODP, Sci. Results. Proc. ODP, Sci. Results, 118. Ocean Drilling Program, College Station, TX, pp. 41–73.

Pallister, J.S., Hopson, C.A., 1981. Samail ophiolite plutonic section: field relations, phase variations, and a model of a spreading ridge magma chamber. J. Geophys. Res. 86, 2593–2644.

Pariso, J., Scott, J.H., Kikawa, E., Johnson, H.P., et al., 1991. A magnetic logging study of Hole 735B gabbros from Hole 735B, Southwest Indian Ridge. In: Von Herzen, R.P., Robinson, P.T., et al., Proc. ODP, Sci. Results, 118. Ocean Drilling Program, College Station, TX, pp. 309–321.

Patriat, Ph., Parson, L.M., 1989. A survey of the Indian Ocean triple junction trace within the Antarctic plate: implications for the junction evolution since 15 Ma. Mar. Geophys. Res. 11, 89–100.

Patriat, Ph., Sauter, D., Munschy, M., Parson, L., 1997. A survey of the Southwest Indian Ridge axis between Atlantis II Fracture Zone and the Indian Ocean triple junction: regional setting and large-scale segmentation. Mar. Geophys. Res. 19, 457–480.

Pettijohn, F.J., 1975. Sedimentary Rocks, 3rd ed. Harper and Row, New York.

Pitcher, W.S., 1993. The Nature and Origin of Granite. Blackie, Glasgow.

Reuber, I., 1991. Geometry and flow pattern of the plutonic sequence of the Salahi massif (Northern Oman ophiolite) — a key to decipher successive magmatic events. In: Peters, T., Nicolas, A., Coleman, R.G. (Eds.), Ophiolite Genesis and the Evolution of the Oceanic Lithosphere. Kluwer Academic Publishers, Dordrecht, pp. 83–103.

Reynolds, I.M., 1985. The nature and origin of titaniferous magnetite-rich layers in the upper zone of the Bushveld Complex: a review and synthesis. Econ. Geol. 80, 1089–1108.

Rhodes, J.M., Dungan, M.A., 1979. The evolution of oceanfloor basaltic magmas. In: Talwani, M., Harrison, C.G.A., Hayes, D.E. (Eds.), Deep Drilling Results in the Atlantic Ocean: Ocean Crust. Maurice Ewing Series 2. American Geophysics Union, Washington, pp. 239–244.

Rhodes, J.M., Dungan, M.A., Blanchard, D.P., Long, P.E., 1979. Magma mixing at mid-ocean ridges: evidence from basalts drilled near 22°N on the Mid-Atlantic Ridge. Tectonophysics 55, 35–61.

Robinson, P.T., Dick, H.J.B., Natland, J.H., in press. Lower oceanic crust formed at an ultra-slow spreading ridge: ODP Hole 735B, Southwest Indian Ridge. In Dilek, Y., Moores, E., Elthon, D., Nicolas, A. (Eds.), Ophiolites and Oceanic Crust: New Insights from Field Studies and Ocean Drilling Programs. Geol. Soc. Am. Special Paper 349.

Robinson, P.T., Von Herzen, R.P., et al., 1989. Proc. ODP, Init. Rep., 118. Ocean Drilling Program, College Station, TX.

Roeder, P., Emslie, R.F., 1970. Olivine–liquid equilibria. Contrib. Mineral. Petrol. 29, 275–289.

Rommeveaux-Jestin, C., Deplus, C., Patriat, P., 1997. Mantle Bouguer anomaly along an ultra-slow spreading ridge: Implications for accretionary processes and comparison with results from the Central Mid-Atlantic Ridge. Mar. Geophys. Res. 19, 481–503.

Rosendahl, B.R., 1976. Evolution of oceanic crust 2: constraints, implications and inferences. J. Geophys. Res. 81, 5305–5314.

Sclater, J.G., Fisher, R.L., Patriat, P., Tapscott, C., Parsons, B., 1981. Eocene to recent development of the Southwest Indian

Ridge, a consequence of the evolution of the Indian Ocean Triple Junction. Geophys. J. R. Astron. Soc. 64, 587–604.

Scoon, R.N., Miatchell, A.A., 1994. Discordant iron-rich ultramafic pegmatites in the Bushveld Complex and their relationship to iron-rich intercumulus and residual liquids. J. Petrol. 35, 881–997.

Severson, M.J., 1991. Geology, mineralization, and geostatistics of the Minnamax/Babbitt Cu–Ni deposit (Local Boy area), Minnesota, Part I: geology. Natural Resources Res. Inst., Univ. Minnesota, Duluth, Tech. Rept., NRRI/Tr-91/13a.

Severson, M.J., Hauck, S.A., 1990. Geology, geochemistry, and stratigraphy of a portion of the Partridge River Intrusion.. Natural Resources Res. Inst., University Minnesota, Duluth, Technical Report, NRRI/GMIN-TR-89-11.

Sinton, J.M., Detrick, R.S., 1992. Mid-ocean ridge magma chambers. J. Geophys. Res. 97, 197–216.

Skolnick, H., 1965. The quartzite problem. J. Sedim. Petrol. 35, 12–21.

Smewing, J.D., Christensen, N.I., Bartholomew, I.D., Browning, P., 1984. The structure of the oceanic upper mantle and lower crust as deduced from the northern section of the Oman ophiolite. Geol. Soc. Lond. Spec. Pub. 13, 41–53.

Stakes, D., Mével, C., Cannat, M., Chaput, T., et al., 1991. Metamorphic stratigraphy of Hole 735B. In: Von Herzen, R.P., Robinson, P.T., et al., Proc. ODP, Sci. Results, 118. Ocean Drilling Program, College Station, TX, pp. 180–254.

Swift, S., Hoskins, H., Stephen, R., 1991. Seismic stratigraphy in a transverse ridge, Atlantis II Fracture Zone. In: Von Herzen, R.P., Robinson, P.T., Proc. ODP, Sci. Results, 118. Ocean Drilling Program, College Station, TX.

Tada, R., Siever, R., 1989. Pressure solution during diagenesis. Annu. Rev. Earth Planet. Sci. 17, 89–118.

Thompson, A., 1959. Pressure solution and porosity. Silica in Sediments, Ireland, H.A. (Ed.). Spec. Publ. Soc. Econ. Paleontol. Mineral. 7, 92–110.

Tucholke, B.E., Lin, J., Kleinrock, M.C., 1998. Megamullions and mullion structure defining oceanic metamorphic core complexes on the Mid-Atlantic Ridge. J. Geophys. Res. 103, 9857–9866.

Usselman, T.M., Hodge, D.S., 1978. Thermal control of low-pressure fractionation processes. J. Volcanol. Geotherm. Res. 4, 265–281.

Vanko, D.A., Stakes, D.S., et al., 1991. Fluids in oceanic layer 3: evidence from veined rocks, Hole 735B, Southwest Indian Ridge. In: Von Herzen, R.P., Robinson, P.T., et al., Proc. ODP, Sci. Results, 118. Ocean Drilling Program, College Station, TX, pp. 181–215.

Viljoen, M.J., Scoon, R.N., 1985. The distribution and main geologic features of discordant bodies of iron-rich ultramafic pegmatite in the Bushveld Complex. Econ. Geol. 80, 1109–1128.

Von Herzen, R.P., Robinson, P.T., et al., 1991. Proc. ODP, Sci. Results, 118. Ocean Drilling Program, College Station, TX.

Wager, L.R., 1963. The mechanism of adcumulus growth in the layered series of the Skaergaard Intrusion. Miner. Soc. Am. Spec. Pap. 1, 1–9.

Wager, L.R., Brown, G.M., 1967. Layered Igneous Rocks. W.H. Freeman, San Francisco.

Wager, L.R., Deer, W.A., 1939. Geological investigations in East Greenland; part 3 — The petrology of the Skaergaard intrusion, Kangerdlugssuaq, East Greenland. Medd. om Grønland 105, 1–352.

Walker, D., Shibata, T., Delong, S.E., 1979. Abyssal tholeiites from the Oceanographer Fracture Zone II. Phase equilibria and mixing. Contrib. Mineral. Petrol. 70, 111–125.

Weyl, P., 1959. Pressure solution and the force of crystallization — a phenomenological theory. J. Geophys. Res. 64, 2001–2025.

Wilson, A.H., 1996. The Great Dyke of Zimbabwe. In: Cawthorn, R.G. (Ed.), Layered Intrusions. Elsevier, Amsterdam, pp. 365–402.

Wilson, D.S., Clague, D.A., Sleep, N.H., Morton, J.L., 1988. Implications of magma convection for the size and temperature of magma chambers at fast spreading ridges. J. Geophys. Res. 93, 11,974–11,984.

Young, I.M., Donaldson, C.H., 1985. Formation of granular-textured layers and laminae within the Rhum crystal pile. Geol. Mag. 122, 519–528.